

Dear Dr. Mirás-Avalos,

Thank you very much for your comments and edits on our manuscript. This really helped a lot modify the paper. I have corrected the suggested edits and some edits as I go through the manuscript again. I have also replied to your comments below.

Hope our submission will be granted.

Thank you very much.

Asim biswas (on behalf of co-authors)

Comments from the Editor:

Non-public comments to the Author:

The revised version of the manuscript with reference NPG-2015-81-R1 and entitled “Fractal behaviour of soil water storage at multiple depths” authored by W. Ji, M. Lin, A. Biswas, B.C. Si, H.W. Chau, and H.P. Cresswell and submitted to the Special Issue “Multifractal analysis in soil systems” to be published in Nonlinear Processes in Geophysics represents a great improvement from the former version submitted to the journal. Authors have addressed the comments and suggestions made by the reviewers.

However, there are still several minor issues to be corrected prior to an eventual publication in the journal. Pleased, check the following pages for further specifications.

Therefore, I still advice for a minor revision prior to the acceptance of the manuscript.

Response: Thank you very much. We have completed the edits in the revised manuscript.

Specific comments to the authors:

Abstract:

Line 16: “deep layers” instead of “deep layer”.

Response: Corrected

Line 17: “The current study” instead of “Current study”.

Response: Corrected

Lines 24-26: “The dynamic nature of...”, this statement is implied in the former two sentences, would you consider removing it, please?

Response: Deleted

Introduction:

Line 46: “other than that of measurement” instead of “other than the scale of measurement”.

Response: Corrected

Line 47: Remove “scale” after “pedon”.

Response: Corrected

Line 48: Remove “scale” after “large catchment”.

Response: Corrected

Line 55: “of the scaling process”.

Response: Corrected

Line 66: “has” instead of “have”.

Response: Corrected

Lines 72-75: “The scaling properties of surface...”, please, consider removing this sentence. If you decide to keep it, please, remove the word “characteristics” after “the same” in line 74.

Response: We kept the sentence but deleted the word.

Line 84: I would use “multifractal approach” instead of “multifractal analysis”.

Response: We have also used approach rather analysis.

Materials and Methods:

Line 91: “differently-sized” instead of “differently sized”.

Response: Corrected

Line 94: “late summer” instead of “later summer”.

Response: Corrected

Line 96: “Variable water” instead of “Variables water”.

Response: Corrected

Line 107: “while deeper layers down to 140 cm were measured” instead of “while the rest deeper soil down to 140 cm depth was measured”.

Response: Corrected

Lines 109-110: “Soil water content data was then multiplied by” instead of “These measured data of soil water content from either the neutron probe or TDR were then multiplied with”.

Response: Modified

Line 117: I think it would be useful to add a couple of citations here, at the end of this sentence.

Response: Citations are added

Lines 197-198: “One of the widely used...”, please, consider re-writing this sentence to “The generalized dimensions were calculated as”.

Response: The sentence is rewritten and separated into two smaller sentences

Line 207: Remove “the” before “D1” and “D0”.

Response: Corrected

Line 225: “was” instead of “is”.

Response: Corrected

Line 240: “represent” instead of “represents”.

Response: Corrected

Line 244: It should be “a contour plot” or “a contour map” instead of just “a contour”.

Response: We used contour plot

Line 249: Please, check this citation, there is no “Biswas and Si, 2012b” in the reference list.

Response: We have added the reference in the list.

Results:

Are units for soil water storage OK? I mean, usually this variable is given in mm and not in cm.

Response: Yes, you are right as often cases the unit used is mm. However, use of cm in presenting soil water storage is also very common when the storage is in higher amount.

Line 252: “the five year period” instead of “five year period”.

Response: Corrected

Line 260: “for the surface layer” instead of “for surface”.

Response: Corrected

Lines 261-265: This is not clear. Do you mean increases and decreases over time or in depth?

Response: We have modified the sentence. It is increase with depth

Line 269: I would use “that” instead of “and”.

Response: Corrected

Line 270: Include “at” before “the deepest layer”.

Response: Added

Lines 275-276: “A similar trend was also observed for the minimum SWS at different layers”. I would remove this sentence since it is already said in the former one.

Response: Deleted

Line 296: “The variability also gradually increased with depth”. Sure? Looking at the table you indicate (Supplementary Table S.3) it seems that variability decreased with depth.

Response: Yes, that was a mistake. We have corrected that.

Line 303: “of three selected dates” instead of “of selected three dates”.

Response: Corrected

Line 305: I do not see what you mean by “SWS trend”.

Response: We have modified the sentence. It is not the SWS trend but the trend of scale invariance.

Line 313: I think that “(single fit)” should be without parenthesis.

Response: Yes, corrected

Lines 321-322: These values are not reported within the supplementary table S.4 as you mentioned here.

Response: table citation deleted

Line 327: Remove “of soil layers”.

Response: Removed

Line 358: Remove “statistically”.

Response: Removed

Lines 358-359: I do not understand why you referred table S.7 in here.

Response: Citation removed

Line 363: “with depth” instead of “with depths”.

Response: Corrected

Line 375: Remove “of measurements”.

Response: Removed

Line 393: “years” instead of “year”.

Response: Corrected

Line 395: “at all depth layers” instead of “at all layers of cumulative depths”.

Response: Corrected

Line 397: Remove “only varied at 3 decimal points”.

Response: Removed

Lines 398-399: Check the subscripts for D1.

Response: Corrected

Lines 409-410: “was also observed at all depth layers” instead of “were also observed at all layers of cumulative depths”.

Response: Corrected

Line 415: “demonstrate” instead of “demonstrates”.

Response: Corrected

Line 417: “those layers” instead of “the layers”.

Response: Corrected

Discussion:

Line 442: “factors” instead of “factor”.

Response: Corrected

Line 473: “Biswas and Si, 2012”, there are a couple of them in the reference list, which one are you referring to?

Response: We have corrected this. There is only Biswas and Si 2012. Rest are Biswas et al. 2012 (a, b, c).

Line 484: Remove “different”.

Response: Removed

Line 487: “values” instead of “value”.

Response: Corrected

Line 509: “exhibit a longer” instead of “exhibit longer”.

Response: Corrected

Line 519: “from the correlation” instead of “from correlation”.

Response: Corrected

Line 535: “and showed stronger similarity to the surface layers”, I would remove this.

Response: Removed

Line 537: “due to the dynamic nature” instead of “due to its dynamic nature”.

Response: Corrected

Lines 541-542: I would remove “with less effect from environment factors”.

Response: Removed

Summary and Conclusions:

I am not sure that this section is needed since it is basically a repetition of the results.

Response: Yes, it summarizes the whole story. Actually that why we say summary and conclusions rather than only conclusions. I think this summarizes the whole paper. So far we kept the summary.

Line 553: “depth” instead of “depths”.

Response: Corrected

Line 560: “those of the deep layers” instead of “that of deep layers”.

Response: Corrected

References:

Lines 583-584: This should be 2012a.

Response: Corrected

Lines 585-587: Since there is no other Biswas et al. 2012, you should remove b after 2012.

Response: Corrected

Lines 588-590: This should be 2012b.

Response: Corrected

Lines 607-609: Why the title of this reference is written in capital letters?

Response: Corrected

Line 636: The “s” should be capital? “Montero, E.S.”?

Response: Corrected

Lines 648-650: Why the title of this reference is written in capital letters?

Response: Corrected

Figure captions:

Figure 1: I would say “over the landscape” instead of “in the different section of landscapes”.

Response: Corrected

Figure 11: This should be the caption for figure 12. In fact, there is no caption that corresponds to figure 11. Please, provide it.

Response: Sorry for this mistake. We have added the title for Fig. 11 and corrected the previous version.

Table 1: Please, consider putting “cm” between parentheses in the title of the table, after “soil water storage” and remove it from the columns “average”, “maximum”, and “minimum”.

Response: Corrected

Table 2: Apart from indicating that the number of data points were the same for all the analyses, you could indicate this number, please.

Response: Corrected

1 Fractal behavior of soil water storage at multiple depths

2 Wenjun Ji¹, Mi Lin¹, Asim Biswas^{1*}, Bing C. Si², Henry W. Chau³, and Hamish P. Cresswell⁴

3 ¹ Department of Natural Resource Sciences, McGill University, 21111 Lakeshore Road, Ste-Anne-de-
4 Bellevue, Quebec, Canada, H9X3V9

5 ² Department of Soil Science, University of Saskatchewan, Saskatchewan, Canada, S7N5A8

6 ³ Department of Soil and Physical Sciences, Lincoln University, PO Box 85084, Lincoln,
7 Christchurch, New Zealand, 7647

8 ⁴ CSIRO Land and Water, Canberra, ACT, Australia, 2601

9 * Correspondence to: A. Biswas (asim.biswas@mcgill.ca Phone: +1 514 398 7620; Fax: +1 514 398
10 7990)

11

12 **Abstract** Spatio-temporal behavior of soil water is essential to understand the science of
13 hydrodynamics. Data intensive measurement of surface soil water using remote sensing has
14 established that the spatial variability of soil water can be described using the principle of
15 self-similarity (scaling properties) or fractal theory. This information can be used in
16 determining land management practices provided the surface scaling properties are kept at
17 deep layers. ~~€The current study examined the scaling properties of sub-surface soil water and~~
18 their relationship to surface soil water, thereby serving as supporting information for plant
19 root and vadose zone models. Soil water storage (SWS) down to 1.4 m depth at seven equal
20 intervals was measured along a transect of 576 m for 5 years in Saskatchewan. The surface
21 SWS showed multifractal nature only during the wet period (from snowmelt until mid to late
22 June) indicating the need for multiple scaling indices in transferring soil water variability
23 information over multiple scales. However, with increasing depth, the SWS became
24 monofractal in nature indicating the need for a single scaling index to upscale/downscale soil
25 water variability information. ~~The dynamic nature of the surface layer soil water in the wet~~
26 ~~period is highly variable compared to the deep layers.~~ In contrast, all soil layers during the
27 dry period (from late June to the end of the growing season in early November) were
28 monofractal in nature, probably resulting from the high evapotranspirative demand of the
29 growing vegetation that surpassed other effects. This strong similarity between the scaling
30 properties at the surface layer and deep layers provides the possibility of inferring about the
31 whole profile soil water dynamics using the scaling properties of the easy-to-measure surface
32 SWS data.

33 **Keywords** Scale invariance, monofractal, multifractal, root zone, remote sensing

34 **1 Introduction**

35 Knowledge on the spatial distribution of soil water over a range of spatial scales and time has
36 important hydrologic applications including assessment of land-atmosphere interactions
37 (Sivapalan, 1992), performance of various engineered covers, monitoring soil water balance
38 and validating various climatic and hydrological models (Rodriguez-Iturbe et al., 1995;Koster
39 et al., 2004). However, high variability in soil is a major challenge in hydrology (Quinn,
40 2004) as the distribution of soil water in the landscape is controlled by various factors and
41 processes operating at different intensities over a variety of extents (Entin et al., 2000). The
42 individual and/or combined influence of these physical factors (e.g. topography, soil
43 properties) and environmental processes (e.g. runoff, evapotranspiration, and snowmelt)
44 gives rise to complex and nested effects, which in turn evolve a signature in the spatial
45 organization (Western et al., 1999) or patterns in soil water as a function of spatial scale
46 (Kachanoski and de Jong, 1988;Kim and Barros, 2002;Biswas and Si, 2011a). This
47 complexity makes the management decision difficult at a scale other than ~~the scale~~that of
48 measurement. Therefore, it is necessary to transfer variability information from one extent
49 (e.g. pedon-~~scale~~) to another (e.g. large catchment-~~scale~~), which is called scaling.

50 The scaling of soil water is possible if the distribution of some statistical parameters (e.g.,
51 variance) remain similar at all studied scopes. This feature, known as scale-invariance, means
52 that the spatial feature in the distribution of soil water will not change if the length scales are
53 multiplied by a common factor (Hu et al., 1997). Generally, the soil water will have a typical
54 size or scale, a value around which individual measurements are centered. So the probability
55 of measuring a particular value will vary inversely as a power of that value, which is known
56 as the power law decay, a typical principle of the scaling process. Now, as the spatial
57 distribution of soil water follows the power law decay (Hu et al., 1997;Kim and Barros,
58 2002;Mascaro et al., 2010), the spatial variability can be investigated and characterized
59 quantitatively over a large range of measurement extents using the fractal theory
60 (Mandelbrot, 1982). When the spatial distribution of soil water is the response of some linear
61 processes, the scaling can be done using a single coefficient over multiple scales and the
62 distribution shows monofractal behavior. However, the spatial distribution of soil water is the
63 nonlinear response of multiple factors and processes acting over a variety of scales and
64 therefore needs multiple scaling indices (multifractals) for quantifying spatial variability (Hu
65 et al., 1997;Kim and Barros, 2002;Mascaro et al., 2010).

66 The multifractal behavior in the surface soil water as a result of temporal evolution of
67 wetting and drying cycles ~~have~~has been reported from a sub-humid environment of
68 Oklahoma by Kim and Barros (2002). Mascaro et al. (2010) reported the multifractal
69 behavior of soil water, which was ascribed as a signature of the rainfall spatial variability.
70 Though these measurements can provide a quick estimate of soil water over a large area, they
71 are limited to very few centimeters of the soil profile. These studies reported the multifractal
72 behavior of only the surface soil water indicating the superficial scaling properties. Surface
73 soil layer is exposed to direct environmental forces and is the most dynamic in nature. The
74 scaling properties of surface soil water can be used for land management practices provided
75 the observed scaling properties remain the same ~~characteristics~~ for the deep layers such as
76 vadose zone or the whole soil profile. Understanding overall hydrological dynamics in soil
77 profile needs information on the scaling properties and the nature of the spatial variability of
78 soil water over a range of scales at deep layers as well (Biswas et al., 2012c). The information
79 on the similarity in the nature of the spatial variability of soil water between the surface layer
80 and deep layers may also help inferring about the soil profile hydrological dynamics.
81 Therefore, the objectives of this study were to examine over time the scaling properties of
82 sub-surface layers and their relationship with surface layers at different initial soil water
83 conditions. We have examined the scaling properties of soil water storage at each layer and
84 their trend with increasing depth from the surface (cumulative depth) over a 5-year period
85 from a hummocky landscape from central Canada using the multifractal ~~analysis~~approach.
86 The relationship between the scaling properties of the surface layer and the subsurface layers
87 was also examined using the joint multifractal analysis.

88 **2 Materials and Methods**

89 **2.1 Study site and data collection**

90 A field experiment was carried out at St. Denis National Wildlife Area (52°12'N latitude,
91 106°50'W longitude and ~549 m above sea level), which is located 40 km east of Saskatoon,
92 Saskatchewan, Canada. The landscape of the study area is hummocky with a complex
93 sequence of slopes (10 to 15%) extending from differently ~~size~~-sized rounded depressions to
94 irregular complex knolls and knobs, a characteristic landscape of the North American Prairie
95 pothole region encompassing approximately 780,000 km² from north-central United States to
96 south-central Canada (National Wetlands Working Group, 1997). Some of these potholes are
97 seasonal in nature meaning to store water in the spring (wet period) and drying out during
98 late summer and in fall season (dry period) (Fig. 1). Variables water distribution within the

99 landscape and in different landform elements such as side slopes, knolls, and depressions
100 support vegetation differently. For example, the large amount of stored water in depressions
101 provide a luxurious supply of water to growing plants compared to knolls (Fig. 1). A transect
102 of 128 points (576 m long) extending in the north-south direction covering multiple knoll-
103 depression cycles was established in 2004 at the study site to examine the soil water variation
104 at field scale. The sample points were selected at 4.5 m regular intervals along the transect to
105 catch the systematic variability of soil water. Soil water measurements were carried out at
106 every 20 cm depth down to 140cm along the transect over the period of 2007 to 2011, among
107 which, the surface soil water (0 to 20 cm) was measured using vertically installed time
108 domain reflectometry (TDR) probes and a metallic cable tester (Model 1502B, Tektronix,
109 Beaverton, OR), while ~~the rest~~ deeper layerssoil down to 140 cm ~~depth-waswere~~ measured
110 using a neutron probe (Model CPN 501 DR Depthprobe, CPN International Inc., Martinez,
111 CA) (Biswas et al., 2012a). ~~These measured data of soil water content from either the neutron~~
112 ~~probe or TDR were~~Soil water content data was then multiplied ~~with-by~~ depth and added
113 together to obtain the overall soil profile water storage so as to examine the fractal behavior
114 of SWS at different depths over time A detailed description of the study site, development of
115 the transect, measurement of soil water and the calibration of measurement instruments can
116 be found in earlier publications from this project (e.g. Biswas et al. (2012a)).

117 **2.2 Data analysis**

118 Various methods including geostatistics (Grego et al., 2006), spectral analysis (Kachanoski
119 and de Jong, 1988), and wavelet analysis (Biswas and Si, 2011a, b) have been used to
120 examine the scale-dependent spatial patterns of SWS. These methods generally deal with
121 how the second moment of SWS changes with scales or frequencies. When the statistical
122 distribution of SWS is normal, the second moment plus the average provide a complete
123 description of the spatial series. However, for other distributions (e.g. left skewed
124 distribution), higher-order moments are necessary for a complete description of the spatial
125 series. For example, let's define the q^{th} moment of a spatial series z as z^q . In this situation, for
126 a positive value of q , the q^{th} moment magnify the effect of larger numbers and diminish the
127 effect of smaller numbers in z . While, on the other hand, for a negative value of q , the q^{th}
128 moment magnify the effect of small numbers and diminish the effect of large numbers in the
129 spatial series z . In this way, using variable moments, we can look at the effect of the
130 magnitude of the data in a series and better characterize its spatial variability.

131 **2.2.1 Statistical self-similarity or scale invariance**

132 Soil water is highly variable in space and time. If the variability in the spatial/temporal
133 distribution remains statistically similar at all studied scales, the SWS is assumed to be self-
134 similar (Evertsz and Mandelbrot, 1992). Self-similarity, also called scale invariance, is
135 closely associated with the transfer of information from one scale to another. We used the
136 multifractal analysis to explore self-similarity or inherent differences in scaling properties of
137 SWS in this study.

138 **2.2.2 Multifractal analysis**

139 On the spatial domain of the studied field, multifractal analysis was used to characterize the
140 scaling property of SWS by statistically measuring the mass distribution (Zelege and Si,
141 2004). The spatial domain or the data along the transect was successively divided into self-
142 similar segments following the rule of the binomial multiplicative cascade (Evertsz and
143 Mandelbrot, 1992). This method required that the two segments divided from a unit interval
144 to be of equal length. With regards to a unit mass M (a normalized probability distribution of
145 a variable or measured in a generalized case) relating to the unit interval, the weight was also
146 partitioned into $[h \times M]$ and $[(1-h) \times M]$, where h was a random variable ($0 \leq h \leq 1$) governed
147 by a probability density function. Sequentially, the new subsets with their associated mass
148 were equally divided into smaller parts. In this way, multifractal analysis was able to describe
149 the scaling properties for the higher-order moments compared to semivariogram which can
150 only measure the scaling properties of the second moment. In a special case, if the scaling
151 properties do not change with q , the spatial series can be identified as monofractal, when one
152 scaling coefficient is enough to characterize scaling property of SWS. Generally, the
153 multifractal analysis is good at measuring the highly fluctuated mass (box size) within a scale
154 interval. This also provides physical insights at all scales regardless of any ad hoc
155 parameterization or homogeneity assumptions in the analysis (Schertzer and Lovejoy, 1987).

156 For SWS spatial series, the scale-invariant mass exponent, was termed as $\tau(q)$ (Liu and
157 Molz (1997):

$$158 \langle [\Delta z(x)]^q \rangle \propto x^{\tau(q)} \quad [1]$$

159 where z was the SWS spatial series, x was the lag distance and the symbol \propto indicated
160 proportionality. The $\tau(q)$ is widely used in multifractal analysis. If the plot of $\tau(q)$ vs. q [or
161 $\tau(q)$ curve] has a single slope (i.e. a linear line), then the series is a simple scaling
162 (monofractal) type. If $\tau(q)$ curve is nonlinear and convex (facing downward), then the series
163 is a multiscaling (multifractal) type. In this study, we used the universal multifractal (UM)

164 model of Schertzer and Lovejoy (1987) to create a reference line that represented the perfect
 165 monofractal type of scaling. Assuming the conservation in mean value of SWS, this model
 166 simulated a cascade process with a scaling function in an empirical moment. It is thus used
 167 here to compare and characterize the observed scaling properties with a reference to the
 168 monofractal behavior. The goodness-of-fit between the $\tau(q)$ curves and the UM model was
 169 tested using the chi-square test. The sum of squared residuals (SSRs) between the $\tau(q)$ curve
 170 and the UM model was also calculated to test the deviation. The $\tau(q)$ curves over the range of
 171 q values (in this study -15 to 15 at 0.5 intervals) were fitted with a linear regression line
 172 (referred to as a single fit). The linear fitting of the $\tau(q)$ curves with $q < 0$ and $q > 0$ (referred to
 173 as segmented fit) was also completed. The difference between the mean of slopes and
 174 segmented fits (for positive and negative q values) was checked using the Student's t test.

175 With similar manner to Eq. [1], the q^{th} order normalized probability measure of SWS,
 176 $\mu_i(q, \varepsilon)$ (also known as the partition function), is proven to vary with the scale size, as below

$$177 \mu_i(q, \varepsilon) = \frac{[p_i(\varepsilon)]^q}{\sum_i [p_i(\varepsilon)]^q} \propto (\varepsilon/L)^{\tau(q)} \quad [2]$$

178 where ε is scale size in the i^{th} segment and $p_i(\varepsilon)$ is the probability of a measure. $p_i(\varepsilon)$ and
 179 measures the concentration of a variable of interest (e.g. SWS) by dividing the value of the
 180 variable in the segment to the whole support length (e.g. to the whole transect of length L
 181 units) (Meneveau et al., 1990; Evertsz and Mandelbrot, 1992). The mass exponent $\tau(q)$ was
 182 related to the probability of mass distribution of SWS.

183 Moreover, the fractal dimension of the subsets of segments in scale size ε was measured
 184 by the multifractal spectrum $f(q)$. When a coarse Hölder exponent (local scaling indices) of α
 185 was in the limit as $\varepsilon \rightarrow 0$, $f(q)$ was calculated as below (Evertsz and Mandelbrot, 1992):

$$186 f(q) = \lim_{\varepsilon \rightarrow 0} \left(\log \left(\frac{\varepsilon}{L} \right) \right)^{-1} \sum_i \mu_i(q, \varepsilon) \log \mu_i(q, \varepsilon) \quad [3]$$

187 and the local scaling indices, α , were given by

$$188 \alpha(q) = \lim_{\varepsilon \rightarrow 0} \left(\log \left(\frac{\varepsilon}{L} \right) \right)^{-1} \sum_i \mu_i(q, \varepsilon) \log p_i(\varepsilon) \quad [4]$$

189 Noting that $f(\alpha)$ was determined through the Legendre transform of the $\tau(q)$ curve:
 190 $f(\alpha) = q\alpha(q) - \tau(q)$ (Chhabra and Jensen, 1989).

191 The multifractal spectrum is a powerful tool in portraying the similarity and/or
 192 differences between the scaling properties of the measures (e.g. SWS). The width of the
 193 spectrum ($\alpha_{\max} - \alpha_{\min}$) was used to examine the heterogeneity in the local scaling indices. The
 194 wider the spectrum, the higher was the heterogeneity in the distribution of SWS and vice
 195 versa. Similarly, the height of the spectrum corresponded to the dimension of the scaling
 196 indices. The small $f(q)$ values indicated rare events (extreme values in the distribution),
 197 whereas the largest value was the capacity dimension (D_0) obtained at $q = 0$.

198 In addition to the multifractal spectrum, [$f(q)$ vs. $\alpha(q)$], for many practical applications,
 199 we used models to incorporate a few selected indicators to describe the scaling property and
 200 variability of a process. One of the widely used models for multifractal measure ~~were~~ was the
 201 generalized dimension ~~s,~~ which ~~The generalized dimension~~ was calculated as below:

$$202 \quad D_q = \frac{1}{q-1} \lim_{\varepsilon \rightarrow 0} \frac{\log \sum_i p_i(\varepsilon)}{\log(\varepsilon)} \quad [5]$$

203 when $q = 1$, D_1 was referred to as the information dimension (also known as entropy
 204 dimension) which provided information about the degree of heterogeneity in the measure
 205 distribution in analogy to the entropy of an open system in thermodynamics (Voss, 1988). If
 206 the value of D_1 is close to unity, it indicated the evenness of measures over the sets of cell
 207 size, while the value approaching 0 indicated a subset of scale in which the irregularities were
 208 concentrated. The D_2 , known as the correlation dimension, was associated with the
 209 correlation function and measured the average distribution density of the SWS (Grassberger
 210 and Procaccia, 1983). For a monofractal distribution, ~~the~~ D_1 and D_2 tend to be equal to ~~the~~
 211 D_0 . The same value of D_0 , D_1 and D_2 indicates that the distribution exhibits perfect self-
 212 similarity and is homogeneous in nature. Contrarily, in multifractal type scaling, the D_1 and
 213 D_2 tend to be smaller than D_0 , showing $D_0 > D_1 > D_2$. Accordingly, the D_1/D_0 value can be
 214 used to describe the heterogeneity in the distribution (Montero, 2005). When this value
 215 equals to 1, it indicated exact monoscaling of the distribution.

216 2.2.3 Joint multifractal analysis

217 While the multifractal analysis characterized the distribution of a SWS spatial series along its
 218 geometric support, the joint multifractal analysis was used to characterize the joint
 219 distribution of two SWS spatial series along a common geometric support. As an extension of
 220 the multifractal analysis, the length of the datasets was also divided into several segments of

221 size ε . Two variables ($P_i(\varepsilon)$ and $R_i(\varepsilon)$ representing two spatial series of SWS) were used
 222 here to measure the probability of the measure in the i^{th} segment, when $P_i(\varepsilon) \propto (\varepsilon/L)^\alpha$ and
 223 $R_i(\varepsilon) \propto (\varepsilon/L)^\beta$. Among them, α and β were the local singularity strength which respectively
 224 represented the mean local exponents of $P_i(\varepsilon)$ and $R_i(\varepsilon)$ in the corresponding expressions
 225 above. The partition function for the joint distribution of $P_i(\varepsilon)$ and $R_i(\varepsilon)$, was calculated as
 226 below (Chhabra and Jensen, 1989; Meneveau et al., 1990; Zeleke and Si, 2004):

$$227 \quad \mu_i(q, t, \varepsilon) = \frac{p_i(\varepsilon)^q \cdot r_i(\varepsilon)^t}{\sum_{j=1}^{N(\varepsilon)} [p_j(\varepsilon)^q \cdot r_j(\varepsilon)^t]}. \quad [6]$$

228 | where the normalized μ ~~is~~ was the partition function, q and t were the real numbers for
 229 weighting. And the aforementioned local singularity strength (coarse Hölder exponents) α
 230 and β were the function to q and t as well:

$$231 \quad \alpha(q, t) = -[\ln(N(\varepsilon))]^{-1} \sum_{i=1}^{N(\varepsilon)} [\mu_i(q, t, \varepsilon) \cdot \ln(p_i(\varepsilon))] \quad [7]$$

$$232 \quad \beta(q, t) = -[\ln(N(\varepsilon))]^{-1} \sum_{i=1}^{N(\varepsilon)} [\mu_i(q, t, \varepsilon) \cdot \ln(r_i(\varepsilon))]. \quad [8]$$

233 To indicate the dimension of the joint distribution, the multifractal spectra $f(\alpha, \beta)$, was
 234 given by

$$235 \quad f(\alpha, \beta) = -[\ln(N(\varepsilon))]^{-1} \sum_{i=1}^{N(\varepsilon)} [\mu_i(q, t, \varepsilon) \cdot \ln(\mu_i(q, t, \varepsilon))]. \quad [9]$$

236 In fact, the joint partition function in Eq. [6] can be simplified to Eq. [2] when q or t is equal
 237 to 0. In this case, the joint multifractal spectrum was transformed to the multifractal spectrum
 238 with a single measure. When both q and t were 0, $f(\alpha, \beta)$ reached maximum and indicated
 239 box dimension of the geometric support of the measures. Pair value of α and β fluctuates with
 240 the change of variable q and t . Therefore, it is possible to examine the distribution of high or
 241 low values (different intensity levels) of one variable with respect to another by varying the
 242 | values of q or t . As the joint multifractal spectra $f(\alpha, \beta)$ represents the frequency of the
 243 occurrence of certain values of α and β , high values of $f(\alpha, \beta)$ represents strong association
 244 between the values of α and β . The Pearson correlation coefficient was used to quantitatively

245 describe their relations across similar moment orders. In addition, correlation coefficients
246 between the surface layer and subsurface layers were used as well to examine the similarity
247 in the scaling properties. Additionally, a contour plot was used to represent the joint
248 distribution of a pair of variables by permuting similar values (highs vs highs or lows vs
249 lows) of q and t . The bottom left part of the contour graph presents the joint distribution of
250 high data values of both variables while top right part represents the low data values of both
251 variables. Therefore, a diagonal contour with low stretch indicate strong association between
252 the variables in consideration (Biswas et al., 2012b).

253 **3 Results**

254 **3.1 Spatial pattern of soil water storage at different depths**

255 Average SWS for the surface 0-20 cm layer over the five year period was 5.51 cm. A slight
256 decrease in SWS was observed at the immediate deep layer (20-40 cm) and a gradual
257 increase thereafter. Five-year average SWS was 5.45 cm, 5.48 cm, 5.56 cm, 5.61 cm, 5.69 cm
258 and 5.77 cm for the 20-40 cm, 40-60 cm, 60-80 cm, 80-100 cm, 100-120 cm and 120-140 cm
259 layers, respectively. Average SWS for a single measurement varied from 3.40 cm to 7.16 cm.
260 The highest average SWS for the surface layer was observed on 29 June 2011. The study area
261 received large amount of spring snowmelt (2010 received 642 mm, double the annual average
262 precipitation) and rainfall during 2011 leading to the high SWS in the surface layer (Weather
263 Canada historical report). The lowest average SWS for the surface layer was observed on 23
264 August 2008, which was one of the driest summers within the five-year study period. The
265 highest average SWS (on 29 June 2011) at the surface layer gradually decreased to 6.55 cm at
266 the deepest layer and the lowest average SWS (on 23 August 2008) at the surface layer
267 gradually increased to 5.28 cm at the 120-140 cm layer (Table 1). These top and bottom
268 boundaries formed a wider range (3.76 cm) of the average SWS at the surface layer compared
269 to that at the deepest layer (1.27 cm). A big range (2.00 cm) in the standard deviation
270 (maximum=2.43 cm and minimum=0.43 cm) of the measurement at the surface layer (0-20
271 cm) was also observed compared to that at the deepest layer (120-140 cm; maximum=1.28
272 and minimum=0.76). This indicated large variations in SWS at the surface layer and-that
273 gradually decreased at deeper layers. The coefficients of variation (CVs) at the surface layer
274 (0-20 cm) varied from 10% to 43% and at the deepest layer (120-140 cm) varied from 13% to
275 23% (Supplementary Table S.1).

276 The maximum SWS at the surface layer also varied widely (maximum=13.96 cm and
277 minimum=4.64 cm) compared to the deepest layer (maximum=9.81 cm and minimum=6.71
278 cm) (Table 1). There was a gradual decrease in the maximum value and increase in the
279 minimum value from the surface to the deepest layer. ~~A similar trend was also observed for~~
280 ~~the minimum SWS at different layers.~~ The maximum SWS at different layers was much
281 localized. For example, there was high SWS at different layers at the locations of 100 to 140
282 m and 225 to 250 m from the origin of the transect. These locations had very high SWS
283 compared to the field-average because they were situated in the depressions while low SWS
284 was observed on the knolls.

285 The variations in SWS with time were evaluated within a year. There was little change in
286 the average SWS over measurements within the years from 2007-2011 except 2008 (Table 1).
287 For example, average SWS was 6.47 cm, 6.03 cm, 6.54 cm, and 6.33 cm on 6 April 2010, 19
288 May 2010, 14 June 2010 and 28 September 2010, respectively. However, the average SWS in
289 2008 drops from 6.28 cm on 2 May 2008 to 3.51 cm on 17 September 2008 in the surface 0-
290 20 cm layer. This falling trend was observed at all soil layers. When compared between
291 years, the trend over time and with depth was very similar in 2007 and 2009 while slightly
292 different between 2010 and 2011 (Table 1). A decreasing trend of the variability was also
293 observed with time. For example, the CV of the surface layer was around 28% on 2 May
294 2008, which gradually decreased to around 13% on 17 September 2008 (Supplementary
295 Table S.1).

296 The average water storage for soil layers with increasing depth was also calculated by
297 adding the individual layers together. The time-averaged values of SWS were 10.96 cm,
298 16.44 cm, 22.00 cm, 27.61 cm, 33.30 cm and 39.07 cm for the 0-40 cm, 0-60 cm, 0-80 cm, 0-
299 100 cm, 0-120 cm and 0-140 cm, respectively (Supplementary Table S.2). The CV of the 0-
300 20 cm layer was the highest during the wet period and gradually declined to the smallest
301 during the dry period (Supplementary Table S.3). The variability also gradually ~~increased~~
302 ~~decreased~~ with depth.

303 **3.2 Statistical scale invariance**

304 The power law relationships and the statistical scale invariance were evaluated using a log-
305 log plot of the aggregated variance of SWS spatial series at different depths of soil layers and
306 the level of disaggregation (or scales) at different q values or statistical moments. The linear
307 relationship of the logarithm of the variance with scale indicated the presence of statistical

308 scale invariance (Fig. 2). The scale invariance was observed for all measurements and at all
309 depths though only all depths of three selected ~~three~~-dates were presented as example. The
310 coefficient of determination (r^2) for a linear fit ($n=7$) was between 0.99 and 1.00 (significant
311 at $P=0.001$) for any measurement days and depths. The-A similar trend in scale invariance
312 was also observed for SWS ~~trend~~-with increasing depths.

313 **3.3 Multifractal analysis**

314 The $\tau(q)$ curves for the surface layer displayed deviation from the UM model during the wet
315 period (Fig. 3). A high SSR value was observed between the $\tau(q)$ curves and the UM model.
316 Nonlinearity in the $\tau(q)$ curve was observed and the slopes of the segmented fit of the $\tau(q)$
317 curves were significantly different from each other. For example, the SSR values between the
318 $\tau(q)$ curve and the UM model were 27.74 and 50.49 for the surface layer (0-20 cm) on 2 May
319 2008 and 31 May 2008, respectively. The slopes of the $\tau(q)$ curve for ~~(single fit)~~ were 0.97
320 and 0.96, respectively for the surface layer of 2 May 2008 and 31 May 2008 (Fig. 3). The
321 slopes of the segmented fit for these measurements were 1.04 ($q<0$) and 0.87 ($q>0$) and, 1.06
322 ($q<0$) and 0.82 ($q>0$), respectively (Fig. 3; Supplementary Table S.4).

323 With the maximum deviation at the surface layer, the $\tau(q)$ curves gradually became very
324 similar to the UM model with depth. The SSR value decreased considerably in deep layers.
325 The slopes of the $\tau(q)$ curve (single fit) became almost unity with no significant difference
326 with the UM model. There was no significant difference between the slopes of the segmented
327 fit. For example, the SSR value was 6.17, 4.98, 8.80, 8.50, 8.86, and 6.16 respectively for the
328 20-40, 40-60, 60-80, 80-100, 100-120, and 120-140 cm layer of 2 May 2008 (~~Supplementary~~
329 ~~Table S.4~~). The slopes (single fit) for these layers were 0.99, 1.00, 1.01, 1.01, 1.00, and 0.99,
330 respectively (Fig. 3). The slopes of the segmented fit were also very close to unity with no
331 significant difference between them.

332 The SSR values gradually decreased and the slopes became almost unity with increasing
333 depth ~~of soil layers~~ (Fig. 4). For example, the SSR values were 14.11, 9.31, 7.71, 6.86, 6.71
334 and 6.30 and the slopes (single fit) were 0.98, 0.99, 0.99, 1.00, 1.00, and 1.00, respectively
335 for 0-40, 0-60, 0-80, 0-100, 0-120 and 0-140 cm layer (Supplementary Table S.5). The slopes
336 of the segmented fit for the $\tau(q)$ curve became almost the same as soil layers went deeper
337 (Fig. 4). The linearity of the $\tau(q)$ curves was gradually strengthened and the SSR value
338 gradually fell with the depth increase of soil layers at any time. A significant difference was
339 observed between the slopes of the $\tau(q)$ curves in segmented fitting at the surface layer of the

340 first three measurements in 2007 (Supplementary Fig. S.1), two measurements in 2008 (Fig.
341 4), three measurements in 2009 and all measurements in 2010 and 2011 (Supplementary Fig.
342 S.2).

343 A decreasing trend in the SSR value was also observed over time within a year. During
344 the dry period, the slopes (single fit and segmented fit) became almost unity with no
345 significant difference (Supplementary Table S.6). For example, the SSR value was 14.12,
346 8.25, 1.30, 1.46, and 0.52 and the slope was 0.99, 0.99, 1.00, 1.00, and 1.00, respectively for
347 the surface layer (0-20 cm) of 21 June 2008, 16 July 2008, 23 August 2008, 17 September
348 2008 and 22 October 2008 (Fig. 3). Similarly, a small SSR value and consistent slope were
349 also observed at the deepest layer (120-140 cm). The SSR values of the 120-140 cm were
350 2.47, 2.47, 3.31, 3.44 and 4.57, respectively for the measurements on 21 June 2008, 16 July
351 2008, 23 August 2008, 17 September 2008 and 22 October 2008 (Supplementary Table S.6).
352 The slope (single fit) for all these measurements was equal to 1.01 (Fig. 3). There was very
353 little difference in the slopes of the segmented fits.

354 A significant difference in the slopes of the segmented fit was observed for the surface
355 layer (0-20 cm) of three measurements in 2007 (17 July, 7 August, and 1 September;
356 Supplementary Fig. S.1), and three measurements in 2009 (21 April, 7 May, and 27 May)
357 (Supplementary Table S.4; Supplementary Fig. S.2). The difference became non-significant
358 with depth and during other measurement times. The trend in deep layers over time was very
359 similar to that of 2008. However, the trend in the SSR values and the slopes with time was
360 different in 2010 and 2011 (Supplementary Table S6). There was very little difference in the
361 SSR values at different times of the year. For example, the SSR value for the surface layer (0-
362 20 cm) was 20.79, 27.18, 24.63 and 26.66 and the slope (single fit) was 0.97, 0.97, 0.97, and
363 0.97, respectively for the measurements on 6 April 2010, 19 May 2010, 14 June 2010, and 28
364 September 2010 (Fig. 3). The slope of the segmented fit of the surface layer (0-20 cm) was
365 statistically significant for all measurements in 2010 and 2011. However, the trend with depth
366 was similar to other years (Supplementary Table S.7).

367 The height of the multifractal spectrum at different depths of measurement was very
368 similar over time. The width of the spectrum ($\alpha_{\max}-\alpha_{\min}$) varied with depth and time (Fig. 5).
369 Generally, a comparative large value of $\alpha_{\max}-\alpha_{\min}$ was observed at the surface layer during the
370 wet period and the value gradually became smaller with depths. For example, the value of
371 $\alpha_{\max}-\alpha_{\min}$ for the surface soil layer (0-20 cm) was 0.23 and 0.31, respectively for the
372 measurements of 2 May 2008 and 31 May 2008 (Fig. 5). Meanwhile, the value of $\alpha_{\max}-\alpha_{\min}$

373 for the soil layers of 20-140 cm with 20 cm increment was 0.15, 0.14, 0.19, 0.20, 0.20, and
374 0.18 for 2 May 2008 and 0.25, 0.19, 0.11, 0.14, 0.12, and 0.11 for 31 May 2008, respectively
375 (Fig. 6). In the later part of the year, the width of the spectrum gradually decreased
376 (Supplementary Table S.8). For example, the $\alpha_{\max}-\alpha_{\min}$ values were 0.19, 0.16, 0.07, 0.08, and
377 0.05, respectively for the surface layer on 21 June 2008, 16 July 2008, 23 August 2008, 17
378 September 2008 and 22 October 2008. Similar trend in values of $\alpha_{\max}-\alpha_{\min}$ was also observed
379 at deep layers (Fig. 6).

380 The trend of the $\alpha_{\max}-\alpha_{\min}$ values in 2007 and 2009 was very similar to that of 2008
381 (Supplementary Table S.8). A higher value of $\alpha_{\max}-\alpha_{\min}$ was observed in the first three
382 measurements of 2007 (Supplementary Fig. S.5) and three measurements of 2009
383 (Supplementary Fig. S.6). However, the values in the surface layer (0-20 cm) ~~of~~
384 ~~measurements~~ in 2010 and 2011 were always higher compared to the deep layers (Fig. 6).
385 There was no decreasing trend in values for the surface layer over time. For example, the
386 $\alpha_{\max}-\alpha_{\min}$ value was 0.21, 0.24, 0.21, and 0.22, respectively for the measurements on 6 April
387 2010, 19 May 2010, 14 June 2010, and 28 September 2010 (Fig. 6). However, the trend in the
388 $\alpha_{\max}-\alpha_{\min}$ value of deep layers was similar to that of other years. A similar trend was observed
389 for cumulative SWS with increasing depth over the years (Fig. 7). Generally, the value of
390 $\alpha_{\max}-\alpha_{\min}$ was also small with the highest in the 0-20 soil layers and gradually decreased with
391 depth (Fig. 7; Supplementary Table S.9).

392 A very similar height of the $f(q)$ curve for all depths and all periods indicated a consistent
393 frequency distribution of the scaling indices (Fig. 6 and 7). Additionally, the position and the
394 symmetry of the curve revealed the distribution of scaling exponents. A symmetric $f(q)$ curve
395 indicated uniform distribution of the scaling exponents. The left side of the spectrum
396 corresponded to the large SWS that were amplified by the positive values of q while the right
397 side indicated smaller SWS that were amplified by negative q values. Symmetry leaning
398 towards the left side during the early spring and in the surface layers in 2008 clearly showed
399 the wider distribution of scaling indices and multifractal nature of the SWS (Fig. 6). While
400 the shifting of the symmetry towards right side clearly indicated less variable scaling indices
401 and thus reduction of multifractal behavior. During the wet years of 2010 and 2011, the
402 symmetry towards left side indicated the variability in the scaling indices. This also persisted
403 with depth. A similar trend was observed for different years at all depth layers ~~of cumulative~~
404 ~~depths~~ (Fig. 7).

405 Generally, the D_1 and D_2 values for different depths of different measurements were very
406 close to 1 (~~only varied at 3 decimal points~~; Fig. 8 and Supplementary Table S.10). In general,
407 the D_1 value of the surface layers gradually increased with depth. Similarly, at any depth, the
408 D_1 values gradually increased from spring to fall season through summer (Fig. 8). Highest
409 variation in D values with q was observed in the surface layer and in the spring season and
410 gradually decreased with depth and later part of the growing season. For example, the first
411 three measurements in 2007 and 2009 presented high D values at high q values
412 (Supplementary Figs. S.9 and S.10). This high D value gradually decreased in the dry period
413 of the year. For example, the D value with positive q was high in the surface layer of 2 May
414 2008 and 31 May 2008 (Fig. 9), whereas it gradually decreased at the later part of the year
415 (e.g. 17 September 2008). The trend with time and depth in 2007 and 2009 was very similar to
416 that of 2008 (Supplementary Tables S.10 and S.11). A consistent high D value was observed
417 in the surface layer for all 2010 and 2011 measurements (Fig. 9). The trend in D values with
418 depth in 2010 and 2011 was also similar to other years. A high value of D_1 and D_2 were also
419 observed at all depth layers ~~of cumulative depths~~ for all measurements (Fig. 10;
420 Supplementary Table S.11).

Formatted: Font: Italic

Formatted: Font: Italic, Subscript

421 **3.4 Joint multifractal analysis**

422 There were strong correlations between the scaling property of the joint distribution of the
423 surface soil layer and the deep soil layers. The narrow width and the diagonally oriented
424 contours between SWS measured on 22 October 2008 at 0-20 cm and 20-40 cm layers clearly
425 demonstrates strong association between those two layers (Fig. 11). The correlation between
426 the surface 0-20 cm and the deep layers on 2 May 2008 (wet period) was larger than 0.9
427 (significant at $P=0.001$; Table 2). The highest correlation was observed between those layers
428 closest to each other. The correlations gradually increased over time and showed high
429 consistency between different layers on 17 September 2008 (Table 2). A very similar trend
430 was observed in other years.

431 **4 Discussion**

432 The amount of water stored in the soil is the result of the dominant underlying hydrological
433 processes. Located in semi-arid climate, the study area receives about 30% of the long term
434 annual average precipitation as snowfall during winter months (Pomeroy et al., 2007).
435 Generally, the depressions receive snow from surrounding uplands or knolls as redistributed
436 by strong prairie wind (Pomeroy and Gray, 1995; Fang and Pomeroy, 2009). The snow melts

437 within a short period of time during the early spring and contributes a large amount of water.
438 The frozen ground restricts infiltration and redistributes excess water within the landscape
439 with greater accumulation in depressions (Fig. 1) (Gray et al., 1985). Apart from the
440 snowmelt, the spring rainfall also contributes to the water inflow in the landscape (Fig. 1).
441 This created a spatial pattern of SWS that was almost a mirror image of the spatial
442 distribution of relative elevation (Biswas and Si, 2011a, c; Biswas et al., 2012a).

443 In the spring, the sources of water loss were the deep drainage and the evaporation. As the
444 loss of water through deep drainage in the study area was as low as 2 to 40 mm per year,
445 occurring mainly through the fractures and preferential flow paths (Hayashi et al., 1998; van
446 der Kamp et al., 2003), the major loss occurred mainly through evaporation from the surface
447 of the bare ground and standing water in depressions. These processes lose a very small
448 amount of water compared to the input of water in spring and early summer leaving the soil
449 wet. Moreover, the surface soil with high organic matter content and low bulk density stored
450 a larger amount of water than the deep layers where the organic matter gradually decreased
451 and the bulk density increased. Reflecting the long-term history of vegetation growth in the
452 landscape, the variability of organic matter content (CV=41%) may be one of the main
453 factors of the high variability in surface layer SWS (Biswas and Si, 2011b).

454 As the vegetation developed in summer, strong evapotranspiration resulted in the lowest
455 average SWS. High amount of water in the depressions allowed grasses to grow faster and
456 transpire more water compared to the knolls (Fig. 1). For example, the aquatic vegetation
457 growth within the depressions was as high as 2 m, while the grasses on the knolls grew to a
458 maximum up to a meter tall. The uneven growth of vegetation and the high
459 evapotranspirative demand in summer narrowed the range of SWS. In the soil where water is
460 more available, evapotranspiration will be stronger while the less evapotranspirative demand
461 will be shown in the relatively dry soil. As a result, the excessive water in the relatively wet
462 soil will be offset by evapotranspiration, reducing the disparities between maximum and
463 minimum values. This variable water uptake was visible in the growth of vegetation in the
464 later part of the growing season as well (Fig. 1). The reduction in the range of SWS was the
465 largest in the surface layer and gradually decreased at deeper layers. This is because the
466 surface layer was exposed to various environmental forces. For example, plants can take up
467 more than 70% of the water they need from the top 50% of the root zone (Feddes et al.,
468 1978). This dynamic behavior of the surface layer exhausted readily available water and

469 finally reduced the range in water storage. This decrease in range also happened in the later
470 part of the growing season.

471 The multifractal and joint multifractal analyses explained the scaling behavior of SWS at
472 different depths over time. The linearity in the log-log plot between the aggregated variance
473 in SWS and the scale at all soil layers over time indicated that SWS behaved under scaling
474 laws (Fig. 2). The near unity slope of the $\tau(q)$ curves and the insignificant difference from the
475 UM model indicated a monofractal type scaling at all layers except the surface layer during
476 the wet period (until mid to late June) where a multifractal behavior led to a slight convex
477 downward curve (Fig. 3). This was also supported by a significant difference between the
478 slope of single and segmented fit in the surface layer during the wet period.

479 Generally during the wet period, excess water fills and drains macropores quickly and
480 creates variations in SWS. Variations in the evaporation due to uneven solar incidence over
481 micro-topography also triggered SWS variability in the surface layer. Additionally, the snow
482 melt and the release of water controlled by local (e.g. soil texture) and non-local (e.g.
483 topography) factors also affected the spatial distribution of SWS, making it more
484 heterogeneous in the wet period (Grayson et al., 1997; Biswas and Si, 2012). Contrarily, as
485 depth increased, less impact of environmental factors tended to create less variability in SWS
486 and exhibited a monofractal behavior which was consistent with the uniform slope shown in
487 Figure 3. During the dry period or later part of the growing season, the SWS storage
488 variability at all depths was small and exhibited monofractal behavior (Fig. 3). Accordingly,
489 the deeper layers in the wet period and all layers in the dry period can be accurately
490 represented by only one scaling exponent while the surface layer in the wet period may
491 require a hierarchy of exponents. A similar trend was observed in SWS of cumulative depth
492 layers (Fig. 4). Resulting from increasingly buffering capacity of the deeper soil layers, the
493 variability of cumulative SWS overlaid the multifractal nature of the surface layer, and finally
494 exhibited monofractal behavior in general.

495 The scaling patterns of SWS at different depths and ~~different~~ periods were further
496 examined using multifractal spectrum [$f(q)$ vs. $\alpha(q)$] (Fig. 6 & Fig. 7). The degree of
497 convexity was used to characterize the heterogeneity of scaling exponents or the degree of
498 multifractality. Large values of $\alpha_{\max}-\alpha_{\min}$ indicated stronger heterogeneity in the local scaling
499 indices of SWS or cumulative SWS and vice versa. The largest value for the surface layer(s)
500 in the wet period indicated the most multifractal behavior of SWS. However, the value
501 decreased with depth and gradually converged in deep layers (Fig. 6). This decline

502 manifested a conformity in the scaling behavior of SWS at deeper layers. Over time, the α_{\max} -
503 α_{\min} value of the surface soil layer decreased and became very similar to that of deep layers.
504 This indicated a reduction in the degree of multifractality for surface soil layers from the wet
505 period to the dry period. A consistent α_{\max} - α_{\min} value for all depths during the dry period
506 suggested the homogeneity and least multifractal nature of SWS. A similar behavior was
507 observed in the cumulative SWS (Fig. 7).

508 To sum up, both the unity slope of the $\tau(q)$ curves (Fig. 3 and Fig. 4) and the degree of
509 convexity of the $f(q)$ spectrum (Fig. 6 & Fig. 7) jointly demonstrated that dynamic behavior
510 of surface soil layers in the wet period made SWS highly variable and exhibited multifractal
511 nature, while less environmental forces and increased buffering capacity of deep layers led to
512 monofractal nature. As a result, multiple scaling exponents were required to characterize the
513 variability of SWS in the surface layer during the wet period, while less number of exponents
514 was necessary for deeper layers during wet period or all layers during dry period.

515 The height of the spectrum, $f(q)$ revealed the dimension or frequency distribution of the
516 scaling indices (Caniego et al., 2003). A low height of $f(q)$ curve indicated rare events or
517 extreme values in the distribution, while a high value represented uniform distribution in all
518 segments. A very similar height of the $f(q)$ curve for all depths and all periods indicated a
519 consistent frequency distribution of the scaling indices.

520 The two upper soil layers during the wet period tended to exhibit a longer tail of the curve
521 on the left, showing more heterogeneity in the distribution of large values. However, when
522 stepping into the dry period, the spectrum tended to display a longer tail on the right
523 compared to the left side, suggesting more heterogeneity in the distribution of smaller values.
524 A few locations with standing water leads to the spatial differences during the wet period
525 while a few points with very small SWS due to high evapotranspiration by growing
526 vegetation during the dry period results in the heterogenic distribution in smaller values.

527 The generalized dimension, D_q was subsequently used to characterize the scaling property
528 and variability in SWS (Fig. 9 and Fig. 10). The largest value of $f(q)$, referred to as the
529 capacity dimension (D_0) obtained at $q = 0$, was close to unity for all layers at different times
530 (Fig. 9). The information dimension (D_1) obtained at $q = 1$ was different from the correlation
531 dimension (D_2), which is denoted as the average distribution density of the measurement for
532 the surface layers in the wet period (Grassberger and Procaccia, 1983). In this case, the
533 different values of D_0 , D_1 and D_2 indicated multifractal nature of the distribution of SWS.

534 Similarly, a non-unity value of D_1/D_0 (Montero, 2005) also indicated the multifractal nature
535 of SWS at the surface layer(s) during the wet period. However, over the growing season, the
536 D_1 and D_2 value approached to D_0 and indicated a monofractal type behavior. Similar values
537 of D_0 , D_1 and D_2 during the dry period also indicated homogeneous distributions.

538 Joint multifractal distribution between the surface to various subsurface layers indicated
539 the similarity in the scaling patterns (Table 2). Basically, the hydrological processes of
540 shallower layers were similar to those of the top layer, while deeper layers showed more
541 disparities from the surface. The nearest subsurface (20-40 cm) layer showed generally the
542 highest similarity with the surface (0-20 cm) layer. However, in the wet period, the
543 subsurface layers displayed the smallest similarity to the surface layer, suggesting a higher
544 dynamic nature of hydrological processes. In the dry period, a stronger effect of vegetation
545 overwhelmed the effect of small variations of water distribution, thus creating a more
546 uniform distribution of SWS at all soil layers ~~and showed stronger similarity to the surface~~
547 ~~layers~~-(Table 2).

548 Overall, our result revealed a multifractal behavior of surface soil layers during the wet
549 period due to ~~its~~the dynamic nature of hydrological processes. This behavior gradually
550 changed with depth and time (Fig. 12). In the deeper layers during the wet period, the
551 behavior became less multifractal or nearly monofractal. Similarly, in the dry period, the
552 vegetation development and its high evapotranspirative demand in the semi-arid climate of
553 the study area increasingly buffered the variation of SWS, as a result, all the soil layers ~~with~~
554 ~~less effect from environment factors~~ showed uniform distribution or monofractal behavior
555 (Fig. 12).

556 **5 Summary and Conclusions**

557 The transformation of information on soil water variability from one scale to another requires
558 knowledge on the scaling behavior and the quantification of scaling indices. Surface soil
559 water can be easily measured (e.g. remote sensing) and presents multi-scaling behavior
560 (requiring multiple scaling indices). However, land-management practices require the
561 understanding of the hydrological dynamics in the root zone and/or the whole soil profile.

562 In this manuscript, the scaling properties of soil water storage at different soil layers
563 measured over a five-year period were examined using multifractal and joint multifractal
564 analysis. The scaling properties of soil water storage mainly suggested a monofractal scaling
565 behavior. However, the surface layer in the wet period or with high soil water storage tended

566 | to be multifractal, which gradually became monofractal with depths. With the decrease in soil
567 | water storage, the scaling behavior became monofractal during the growing season. In he
568 | year with high annual precipitation, the soil stored more water in the surface layer throughout
569 | the growing period and displayed nearly multifractal scaling behavior. This multifractal
570 | nature indicated that the transformation of information from one scale to another at the
571 | surface layer during the wet period requires multiple scaling indices. On the contrary, the
572 | transformation requires a single scaling index during the dry period for the whole soil profile.
573 | The scaling properties of the surface layer were highly correlated with ~~that~~ those of the deep
574 | layers, which indicated a highly similar scaling behavior in the soil profile. The study was
575 | conducted in an undulating landscape from a semi-arid climate and the results were very
576 | consistent over the years. Therefore, the observation completed at the field scale in this type
577 | of landscape and climate may be generalized in similar landscapes and climatic situations,
578 | otherwise may need to be examined thoroughly. The method used here can be transferred to
579 | examine the scaling properties in other experimental situations.

580 | **6 Acknowledgements**

581 | The project was funded by the Natural Science and Engineering Research Council of Canada.
582 | The help from the graduate student and the summer students of the Department of Soil
583 | Science at the University of Saskatchewan in collecting field data is highly appreciated.

584 | **7 References**

- 585 | Biswas, A., and Si, B. C.: Scales and locations of time stability of soil water storage in a
586 | hummocky landscape, *J. Hydrol.*, 408, 100-112, 10.1016/j.jhydrol.2011.07.027, 2011a.
587 | Biswas, A., and Si, B. C.: Identifying scale specific controls of soil water storage in a
588 | hummocky landscape using wavelet coherency, *Geoderma*, 165, 50-59,
589 | 10.1016/j.geoderma.2011.07.002, 2011b.
590 | Biswas, A., and Si, B. C.: Revealing the Controls of Soil Water Storage at Different Scales in
591 | a Hummocky Landscape, *Soil Science Society of America Journal*, 75, 1295-1306,
592 | 10.2136/sssaj2010.0131, 2011c.
593 | Biswas, A., Chau, H. W., Bedard-Haughn, A. K., and Si, B. C.: Factors controlling soil water
594 | storage in the hummocky landscape of the Prairie Pothole Region of North America,
595 | *Canadian Journal of Soil Science*, 92, 649-663, 10.4141/cjss2011-045, 2012a.
596 | Biswas, A., Cresswell, H. P., and Si, B. C.: Application of Multifractal and Joint Multifractal
597 | Analysis in Examining Soil Spatial Variation: A Review, in: *Fractal Analysis and Chaos*
598 | in Geosciences, edited by: Ouadfeul, S.-A., InTech, Croatia, 109-138, 2012b.
599 | Biswas, A., and Si, B. C.: Identifying effects of local and nonlocal factors of soil water
600 | storage using cyclical correlation analysis, *Hydrological Processes*, 26, 3669-3677,
601 | 10.1002/hyp.8459, 2012.
602 | Biswas, A., Zeleke, T. B., and Si, B. C.: Multifractal detrended fluctuation analysis in
603 | examining scaling properties of the spatial patterns of soil water storage, *Nonlinear*
604 | *Processes in Geophysics*, 19, 227-238, 10.5194/npg-19-227-2012, 2012c.

Formatted: Indent: Left: 0 cm,
Hanging: 0.63 cm

Field Code Changed

Formatted: Font: Times New Roman,
12 pt

605 Chhabra, A., and Jensen, R. V.: Direct determination of the $f(\alpha)$ singularity spectrum,
606 Physical Review Letters, 62, 1327-1330, 1989.

607 Entin, J. K., Robock, A., Vinnikov, K. Y., Hollinger, S. E., Liu, S. X., and Namkhai, A.:
608 Temporal and spatial scales of observed soil moisture variations in the extratropics,
609 Journal of Geophysical Research-Atmospheres, 105, 11865-11877,
610 10.1029/2000jd900051, 2000.

611 Evertsz, C. J. G., and Mandelbrot, B. B.: Self-similarity of harmonic measure on DLA,
612 Physica A: Statistical Mechanics and its Applications, 185, 77-86,
613 [http://dx.doi.org/10.1016/0378-4371\(92\)90440-2](http://dx.doi.org/10.1016/0378-4371(92)90440-2), 1992.

614 Fang, X., and Pomeroy, J. W.: Modelling blowing snow redistribution to prairie wetlands,
615 Hydrological Processes, 23, 2557-2569, 10.1002/hyp.7348, 2009.

616 Feddes, R. A., Kowalik, P. J., and Zaradny, H.: Simulation of field water use and crop yield.,
617 John Wiley & Sons Inc., New York, 1978.

618 Grassberger, P., and Procaccia, I.: Characterization of Strange Attractors, Physical Review
619 Letters, 50, 346-349, 1983.

620 Gray, D. M., Landine, P. G., and Granger, R. J.: Simulating infiltration into frozen Prairie
621 soils in streamflow models, Canadian Journal of Earth Sciences, 22, 464-472, 1985.

622 Grayson, R. B., Western, A. W., Chiew, F. H. S., and Bloschl, G.: Preferred states in spatial
623 soil moisture patterns: Local and nonlocal controls, Water Resources Research, 33, 2897-
624 2908, 1997.

625 Grego, C. R., Vieira, S. R., Antonio, A. M., and Della Rosa, S. C.: Geostatistical analysis for
626 soil moisture content under the no tillage cropping system, Scientia Agricola, 63, 341-
627 350, 2006.

628 Hayashi, M., van der Kamp, G., and Rudolph, D. L.: Water and solute transfer between a
629 prairie wetland and adjacent uplands, 2. Chloride cycle, J. Hydrol., 207, 56-67, 1998.

630 Hu, Z. L., Islam, S., and Cheng, Y. Z.: Statistical characterization of remotely sensed soil
631 moisture images, Remote Sensing of Environment, 61, 310-318, 1997.

632 Kachanoski, R. G., and de Jong, E.: Scale dependence and the temporal persistence of spatial
633 patterns of soil water storage, Water Resources Research, 24, 85-91,
634 10.1029/WR024i001p00085, 1988.

635 Kim, G., and Barros, A. P.: Downscaling of remotely sensed soil moisture with a modified
636 fractal interpolation method using contraction mapping and ancillary data, Remote
637 Sensing of Environment, 83, 400-413, 2002.

638 Koster, R. D., Dirmeyer, P. A., Guo, Z. C., Bonan, G., Chan, E., Cox, P., Gordon, C. T.,
639 Kanae, S., Kowalczyk, E., Lawrence, D., Liu, P., Lu, C. H., Malyshev, S., McAvaney, B.,
640 Mitchell, K., Mocko, D., Oki, T., Oleson, K., Pitman, A., Sud, Y. C., Taylor, C. M.,
641 Verseghy, D., Vasic, R., Xue, Y. K., Yamada, T., and Team, G.: Regions of strong
642 coupling between soil moisture and precipitation, Science, 305, 1138-1140,
643 10.1126/science.1100217, 2004.

644 Liu, H. H., and Molz, F. J.: Multifractal analyses of hydraulic conductivity distributions,
645 Water Resources Research, 33, 2483-2488, 10.1029/97WR02188, 1997.

646 Mandelbrot, B. B.: The fractal geometry of nature, W.H. Freeman and Company, San
647 Francisco, 1982.

648 Mascaro, G., Vivoni, E. R., and Deidda, R.: Downscaling soil moisture in the southern Great
649 Plains through a calibrated multifractal model for land surface modeling applications,
650 Water Resources Research, 46, W08546, 10.1029/2009WR008855, 2010.

651 Meneveau, C., Sreenivasan, K. R., Kailasnath, P., and Fan, M. S.: Joint multifractal
652 measures: Theory and applications to turbulence, Physical Review A, 41, 894-913, 1990.

653 Montero, E. S.: Rényi dimensions analysis of soil particle-size distributions, Ecological
654 Modelling, 182, 305-315, <http://dx.doi.org/10.1016/j.ecolmodel.2004.04.007>, 2005.

Formatted: Font: Times New Roman,
12 pt

- 655 National Wetlands Working Group: The Canadian wetland classification system, University
656 of Waterloo, ON, 1997.
- 657 Pomeroy, J. W., and Gray, D. M.: Snowcover, accumulation, relocation, and management, in:
658 NHRI Science Report No. 7, Environment Canada, Saskatoon, SK., 144, 1995.
- 659 Pomeroy, J. W., de Boer, D., and Martz, L. W.: Hydrology and water resources, in:
660 Saskatchewan: Geographic Perspectives, edited by: Thraves, B., CRRC, Regina, SK,
661 Canada, 2007.
- 662 Quinn, P.: Scale appropriate modelling: representing cause-and-effect relationships in nitrate
663 pollution at the catchment scale for the purpose of catchment scale planning, *J. Hydrol.*,
664 291, 197-217, 10.1016/j.hydrol.2003.12.040, 2004.
- 665 Rodriguez-Iturbe, I., Vogel, G. K., Rigon, R., Entekhabi, D., Castelli, F., and Rinaldo, A.: On
666 the spatial-organization of soil-moisture fields, *Geophysical Research Letters*, 22, 2757-
667 2760, 10.1029/95gl02779, 1995.
- 668 Schertzer, D., and Lovejoy, S.: Physical modeling and analysis of rain and clouds by
669 anisotropic scaling multiplicative processes, *Journal of Geophysical Research:*
670 *Atmospheres*, 92, 9693-9714, 10.1029/JD092iD08p09693, 1987.
- 671 Sivapalan, M.: Scaling of hydrologic parameterizations, 1. Simple models for the scaling of
672 hydrologic state variables, examples and a case study, Center for Water Research,
673 University of Western Australia, Nedlands, WA, Australia, 1992.
- 674 van der Kamp, G., Hayashi, M., and Gallen, D.: Comparing the hydrology of grassed and
675 cultivated catchments in the semi-arid Canadian prairies, *Hydrological Processes*, 17,
676 559-575, 10.1002/hyp.1157, 2003.
- 677 Voss, R.: Fractals in nature: From characterization to simulation, in: *The Science of Fractal*
678 *Images*, edited by: Peitgen, H.-O., and Saupe, D., Springer New York, 21-70, 1988.
- 679 Western, A. W., Grayson, R. B., Bloschl, G., Willgoose, G. R., and McMahon, T. A.:
680 Observed spatial organization of soil moisture and its relation to terrain indices, *Water*
681 *Resources Research*, 35, 797-810, 1999.
- 682 Zeleke, T. B., and Si, B. C.: Scaling properties of topographic indices and crop yield:
683 Multifractal and joint multifractal approaches, *Agronomy Journal*, 96, 1082-1090, 2004.

684

685 **Figure captions**

686 Fig. 1: Conceptual schematics showing the vegetation growth patterns ~~in the different section~~
687 ~~o~~ver the landscapes at different times of the year. The figure is developed based on field
688 observations and the scale is arbitrary.

689 Fig. 2. Log-log plot between the aggregated variance of the SWS spatial series and the scale.
690 A linear relationship indicated the presence of scale invariance and scaling laws for three
691 selected dates.

692 Fig. 3. Mass exponents for soil water storage spatial series measured at selected 20 cm soil
693 layer down to 140 cm in 2008 for a range of q (-15 to 15 at 0.5 increments). The solid line is a
694 linear reference created following the UM model of Schertzer and Lovejoy (1987) passing
695 through ($q = 0$).

696 Fig. 4. Mass exponents for selected soil water storage spatial series from surface to different
697 soil layers (cumulative storage) at 20 cm increment down to 140 cm in 2008 for a range of q
698 (-15 to 15 at 0.5 increments). The solid line is a linear reference created following the UM
699 model of Schertzer and Lovejoy (1987) passing through ($q = 0$).

700 Fig. 5. The width of the multifractal spectrum ($\alpha_{\max} - \alpha_{\min}$ value) for soil water storage at different
701 depths (20 cm increment) for all measurements completed during the study period.

702 Fig. 6. Multifractal spectra of soil water storage spatial series measured at each 20 cm soil
703 layer down to 140 cm in 2008, 2010 and 2011 for a range of q (-15 to 15 at 0.5 increments).

704 Fig. 7. Multifractal spectra of soil water storage spatial series from surface to different soil
705 layers (cumulative storage) at 20 cm increment down to 140 cm in 2008, 2010 and 2011 for a
706 range of q (-15 to 15 at 0.5 increments).

707 Fig. 8. The information dimension (D1) for soil water storage at different depths (20 cm
708 increment) over the whole measurement period.

709 Fig. 9. Generalized dimension spectra of soil water storage spatial series measured at each 20
710 cm soil layer down to 140 cm in 2008 for a range of q (-15 to 15 at 0.5 increments).

711 Fig. 10. Generalized dimension spectra of soil water storage spatial series from surface to
712 different soil layers (cumulative storage) at 20 cm increment down to 140 cm in 2008 for a
713 range of q (-15 to 15 at 0.5 increments).

714 Fig. 11: Multifractal spectra of joint distribution of SWS at 0-20 cm and 20-40 cm measured
715 on 22 October 2008. Contour lines show the joint scaling dimensions of the SWS
716 measurement series.

717 Fig. 11: Conceptual schematics showing vegetation development over time, dominant water
718 loss processes and the scaling behavior of soil water storage at different depths. The figure is
719 developed based on field observations and scaling analysis. The scale of the figure is
720 arbitrary.

721 Tables

722 Table 1

Table 1. Maximum, minimum, and average soil water storage (cm) at different depths (20 cm increment) over the whole measurement period.

	0-20 cm			20-40 cm			40-60 cm			60-80 cm			80-100 cm			100-120 cm			120-140 cm		
	Maximum (cm)	Minimum (cm)	Average (cm)	Maximum (cm)	Minimum (cm)	Average (cm)	Maximum (cm)	Minimum (cm)	Average (cm)	Maximum (cm)	Minimum (cm)	Average (cm)	Maximum (cm)	Minimum (cm)	Average (cm)	Maximum (cm)	Minimum (cm)	Average (cm)	Maximum (cm)	Minimum (cm)	Average (cm)
Jul 17 2007	13.96	3.25	5.65	11.55	3.09	5.63	9.43	2.59	5.73	9.06	3.34	5.90	9.51	3.22	5.89	9.81	3.55	6.05	9.81	3.54	6.14
Aug 7 2007	13.96	3.05	4.90	9.28	2.73	5.04	8.30	2.40	5.21	9.36	2.75	5.48	8.23	2.96	5.57	7.52	3.17	5.62	9.11	3.17	5.67
Sept 1 2007	13.96	2.26	5.29	9.28	3.00	5.08	8.08	2.42	5.23	6.98	2.75	5.38	7.17	2.92	5.52	8.08	3.20	5.64	9.07	3.23	5.73
Oct 12 2007	8.30	3.40	5.04	6.92	3.07	5.03	6.74	2.43	5.19	7.60	2.81	5.36	8.39	2.93	5.48	7.92	3.25	5.60	8.55	3.25	5.67
May 2 2008	13.96	4.49	6.28	9.96	4.09	6.03	9.43	3.69	5.80	8.83	3.16	5.74	9.51	2.90	5.66	9.81	3.26	5.70	9.81	3.30	5.75
May 31 2008	13.96	3.30	5.21	9.28	1.54	5.51	8.08	1.58	5.55	6.85	3.00	5.58	7.08	3.08	5.64	8.08	3.22	5.70	8.39	3.25	5.79
Jun 21 2008	8.77	3.06	4.70	7.84	3.43	5.25	6.86	2.80	5.38	6.78	2.77	5.52	7.08	3.04	5.61	7.73	3.28	5.69	8.48	3.23	5.77
July 16 2008	7.07	2.78	4.03	6.78	3.06	4.77	6.71	2.60	5.10	6.75	2.56	5.30	6.84	2.91	5.43	6.98	3.17	5.56	7.01	3.16	5.64
Aug 23 2008	4.96	2.44	3.40	5.66	2.73	4.11	6.02	2.37	4.59	6.44	2.36	4.90	6.56	2.63	5.12	6.85	3.04	5.30	6.81	2.99	5.42
Sept 17 2008	4.64	2.66	3.51	5.63	2.79	4.07	5.91	2.49	4.55	6.28	2.45	4.85	6.59	2.63	5.05	6.68	3.05	5.25	6.91	2.96	5.37
Oct 22 2008	6.11	3.83	4.96	6.03	3.10	4.37	5.92	2.52	4.53	6.13	2.46	4.79	6.55	2.63	5.00	6.61	3.00	5.18	6.73	1.22	5.28
April 20 2009	13.96	4.73	6.67	11.55	3.62	5.84	10.49	3.23	5.62	8.83	2.97	5.48	9.51	2.67	5.38	9.81	3.08	5.49	9.81	2.85	5.66
May 7 2009	13.96	4.45	5.97	9.51	3.68	5.70	8.08	3.26	5.49	8.30	3.00	5.36	7.85	2.73	5.35	9.81	3.01	5.43	8.91	2.84	5.51
May 27 2009	12.60	3.67	5.43	8.15	3.55	5.52	8.08	3.43	5.39	6.78	3.13	5.37	7.16	2.64	5.39	8.08	2.96	5.51	8.45	2.80	5.53
July 21 2009	6.92	3.16	4.56	7.24	3.16	4.83	6.55	2.91	5.00	6.72	2.95	5.23	6.77	2.58	5.24	6.91	3.02	5.34	6.89	3.24	5.43
Aug 27 2009	6.64	3.42	5.01	6.67	3.57	5.07	6.32	2.84	4.92	6.50	2.85	5.03	6.76	2.57	5.16	6.79	3.00	5.25	6.90	3.02	5.34
Oct 27 2009	6.65	3.89	5.30	6.44	3.44	4.90	6.04	2.74	4.80	6.36	2.68	4.91	6.55	2.60	5.05	6.71	3.05	5.17	6.71	2.79	5.29
April 6 2010	13.96	4.67	6.47	9.51	3.53	5.52	9.43	3.19	5.31	8.83	2.91	5.35	9.51	2.61	5.23	9.81	3.01	5.34	9.81	2.83	5.41
May 19 2010	13.96	4.08	6.04	11.32	4.28	5.94	10.49	4.46	5.94	8.75	4.08	5.93	8.60	3.55	5.90	9.81	4.03	5.91	9.81	3.96	5.85
June 14 2010	13.96	4.38	6.54	11.55	4.48	6.32	10.49	4.58	6.31	8.83	4.27	6.29	9.51	3.86	6.22	9.81	4.37	6.24	9.81	4.50	6.20
Sept 28, 2010	13.96	4.51	6.33	11.55	4.48	6.16	9.43	3.77	6.08	8.83	3.91	6.13	9.51	3.83	6.12	9.81	4.11	6.16	9.79	4.18	6.20
May 13, 2011	13.96	4.82	7.12	11.55	4.87	6.61	10.49	4.75	6.50	9.21	4.54	6.40	9.51	4.16	6.34	9.96	3.17	6.32	9.79	4.30	6.45
Jun 6, 2011	13.96	4.31	7.05	11.55	4.56	6.59	10.49	3.85	6.52	9.06	4.75	6.44	9.51	4.21	6.40	9.96	3.17	6.39	9.79	4.77	6.52
Jun 29, 2011	13.96	4.93	7.16	11.55	4.96	6.73	10.49	4.29	6.64	9.74	4.42	6.57	9.51	4.28	6.49	9.96	3.17	6.46	9.79	4.30	6.55
Sept 29, 2011	12.60	3.11	5.25	8.15	3.46	5.50	8.08	2.88	5.68	7.58	4.03	5.82	9.19	3.77	5.89	9.51	3.81	6.02	9.36	4.14	6.04
5 year average			5.51			5.45			5.48			5.56			5.61			5.69			5.77

725 Table 2: Correlation coefficients between joint multifractal indices (α and β) (n=440) of the
 726 surface layer with those from subsurface layers at 20cm intervals in 2008. ~~The number of~~
 727 ~~data points are same for all the analysis.~~

	2 May 2008	31 May 2008	21 Jun. 2008	16 Jul. 2008	23 Aug. 2008	17 Sep. 2008	22 Oct. 2008
0-20 cm vs. 20-40 cm	0.96	0.98	0.99	0.99	0.99	1.00	1.00
0-20 cm vs. 40-60 cm	0.93	0.96	0.96	0.97	0.97	1.00	1.00
0-20 cm vs. 60-80 cm	0.93	0.94	0.95	0.95	0.96	0.99	0.99
0-20 cm vs. 80-100 cm	0.92	0.92	0.93	0.94	0.94	0.98	0.99
0-20 cm vs. 100-120 cm	0.92	0.92	0.93	0.93	0.93	0.97	0.99
0-20 cm vs. 120-140 cm	0.93	0.94	0.95	0.94	0.94	1.00	1.00

728

729

730

731

732

733

734

735

736

737

738

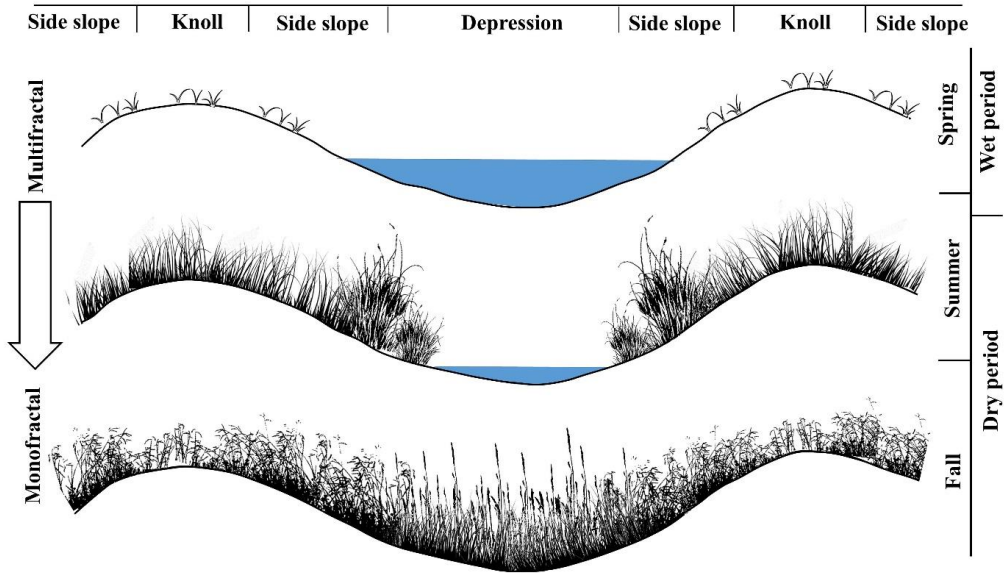
739

740

741

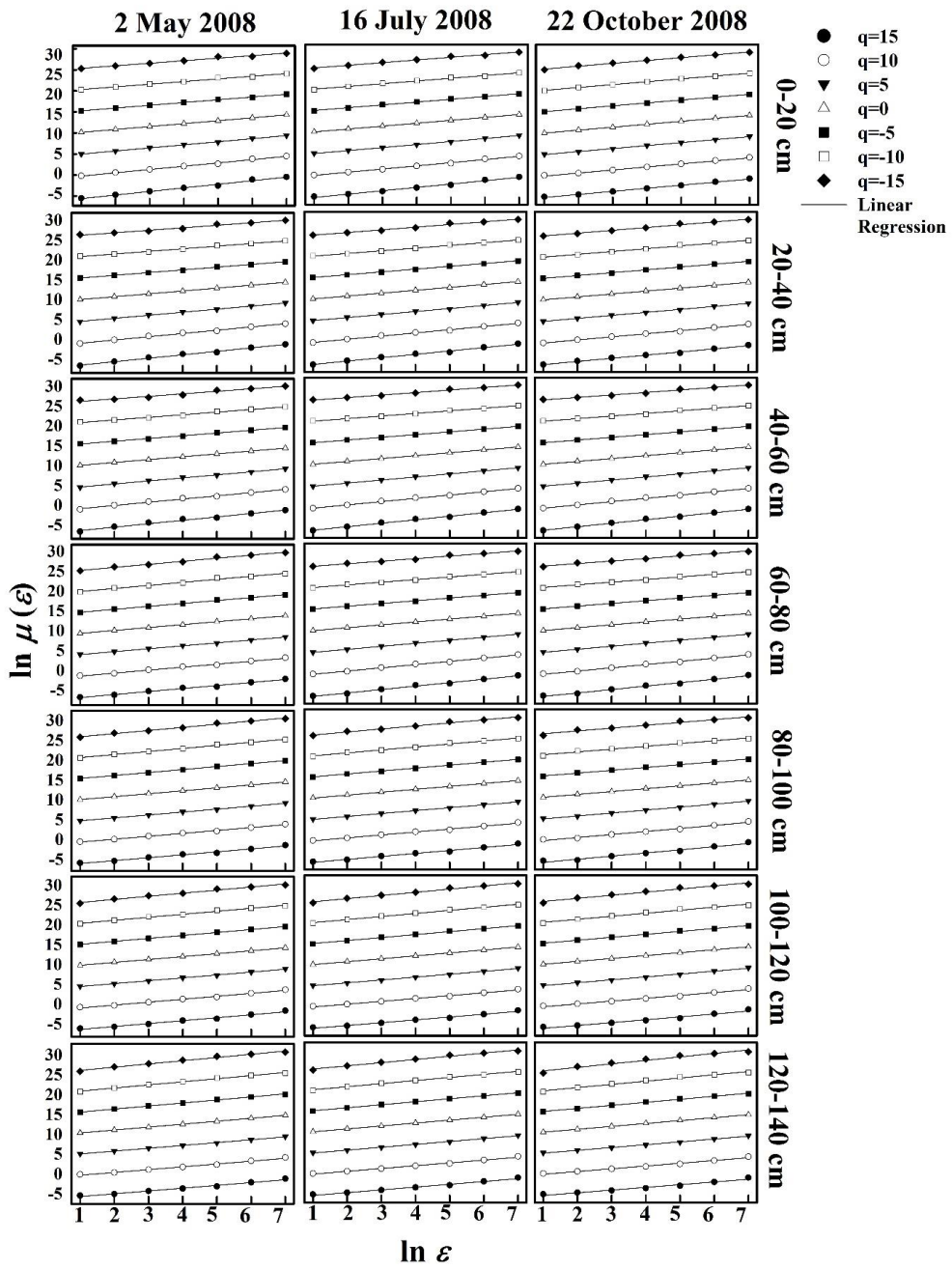
742

743 **Figures**



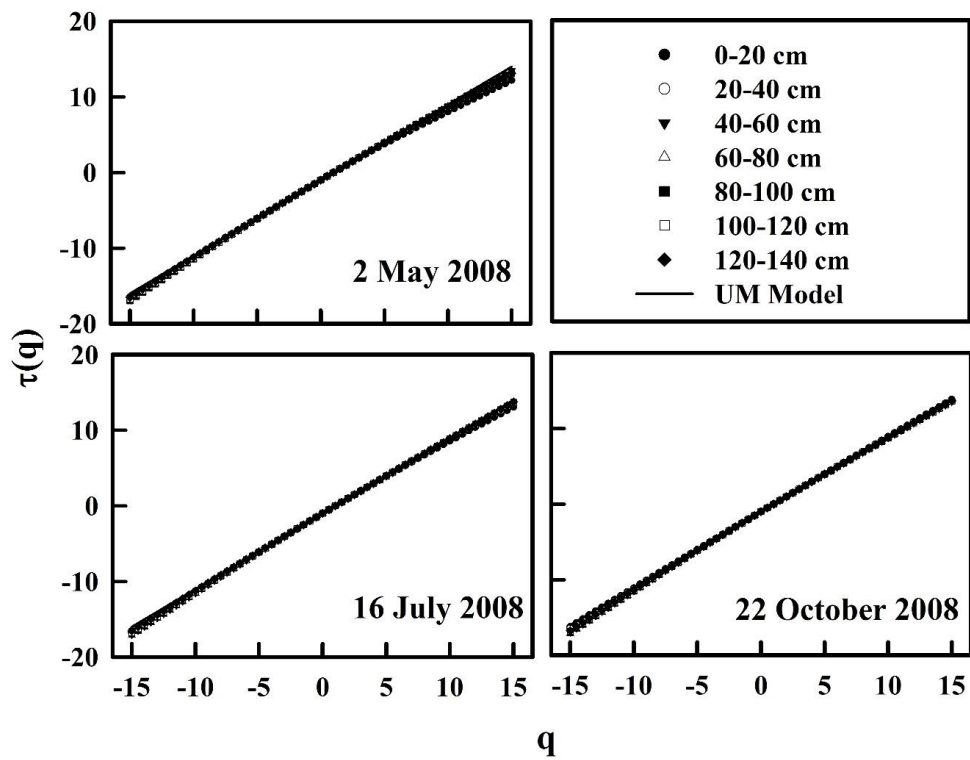
744

745 **Figure 1**



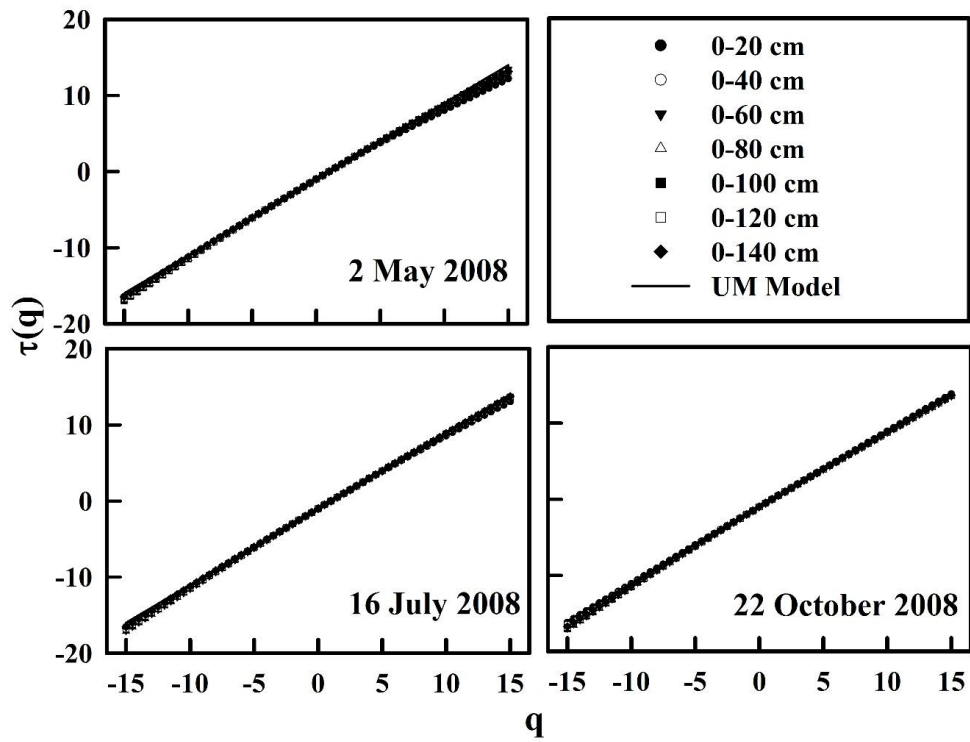
746

747 Figure 2



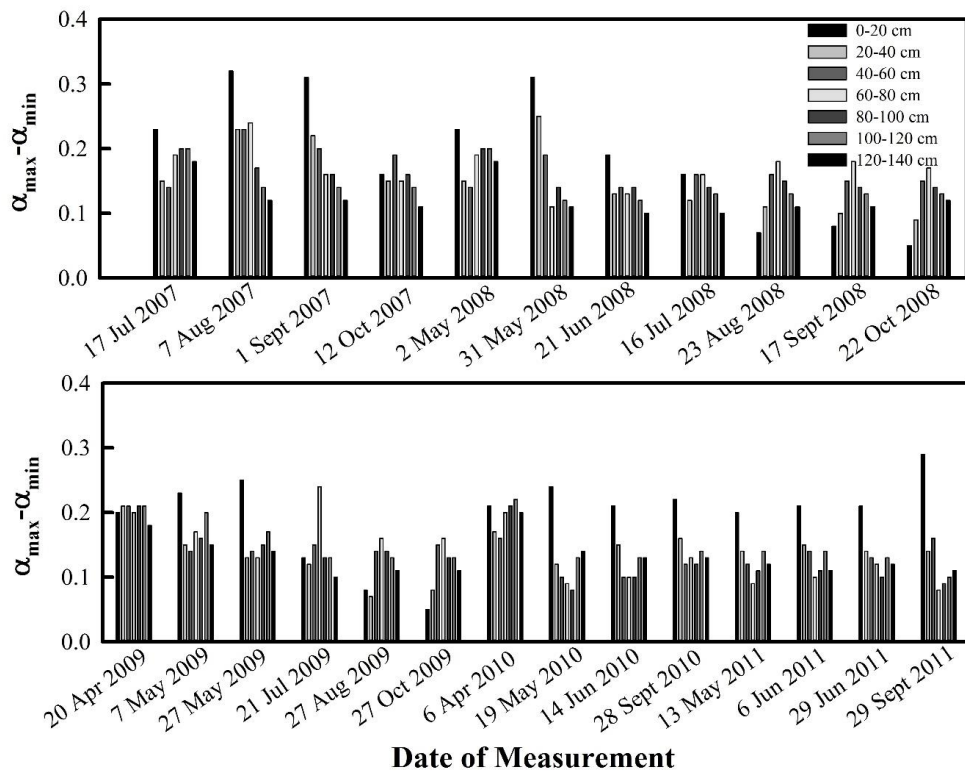
748

749 Figure 3



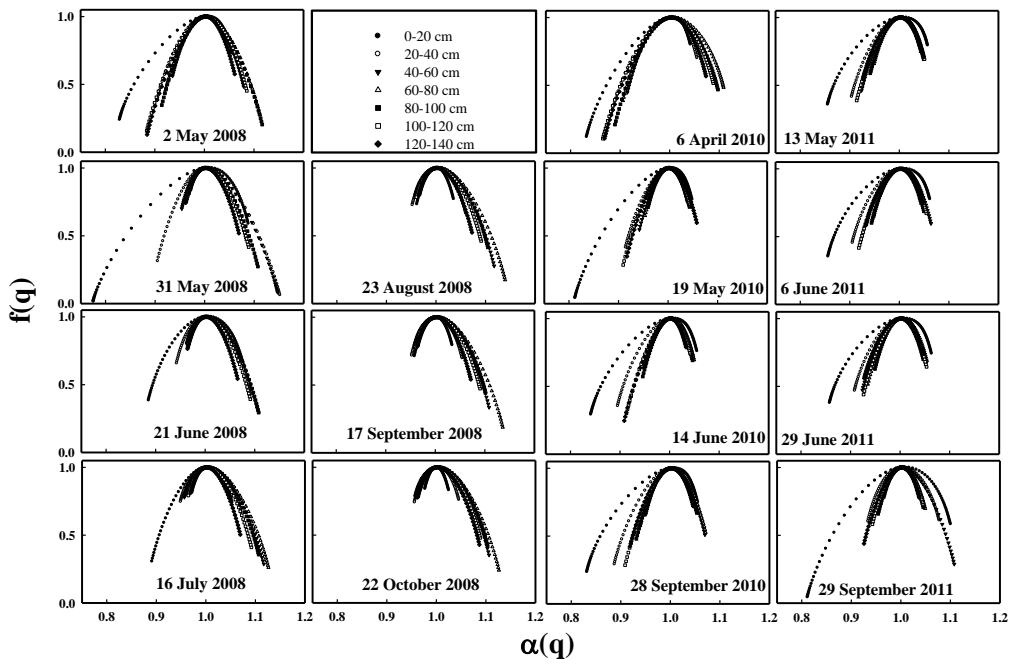
750

751 Figure 4



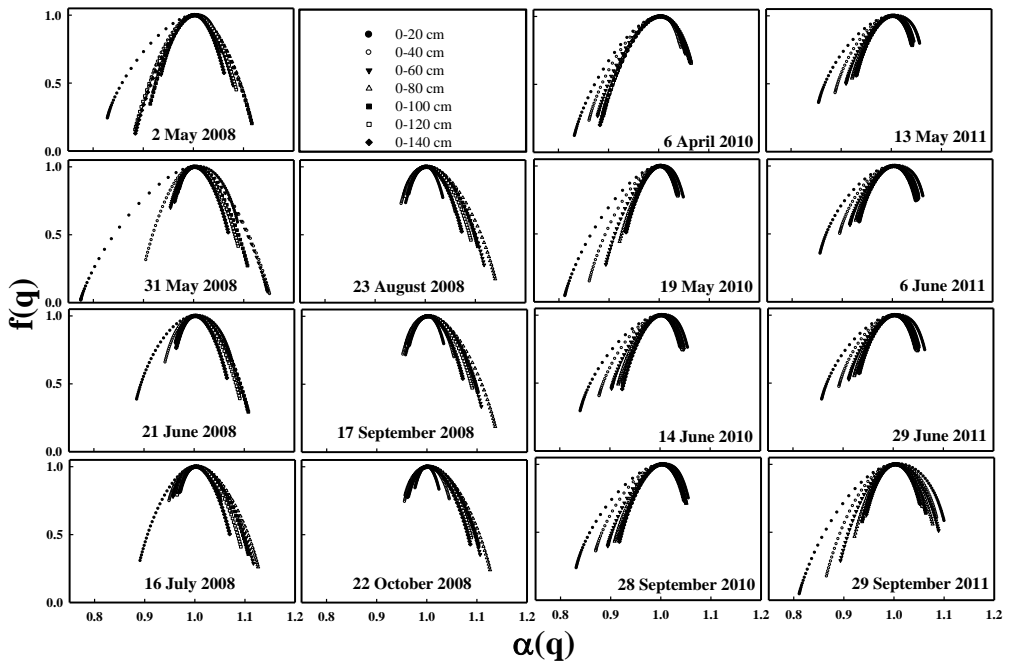
752

753 Figure 5



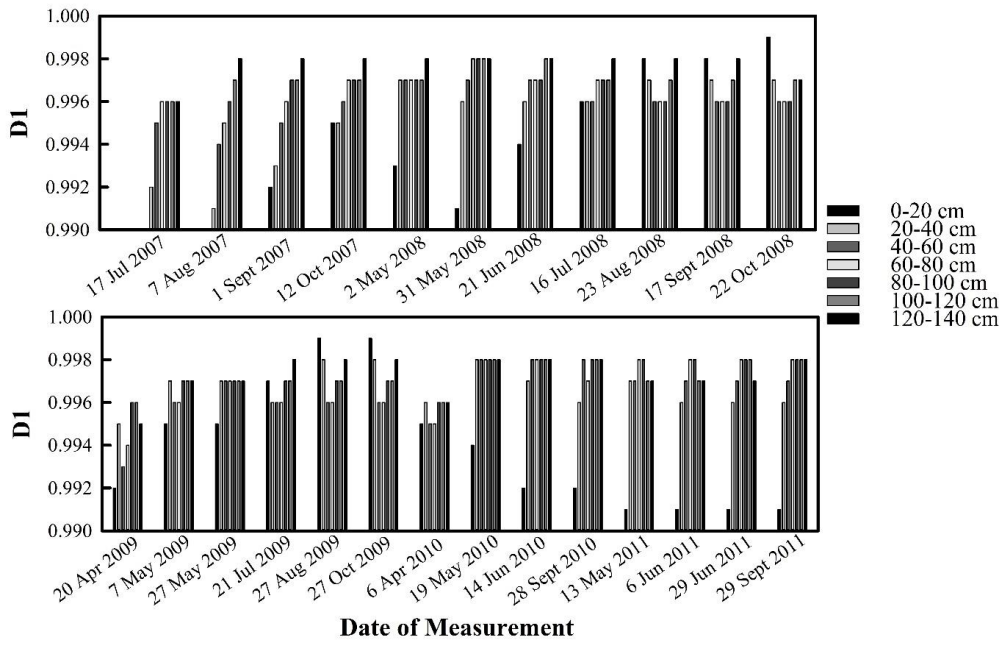
754
755

756 Figure 6



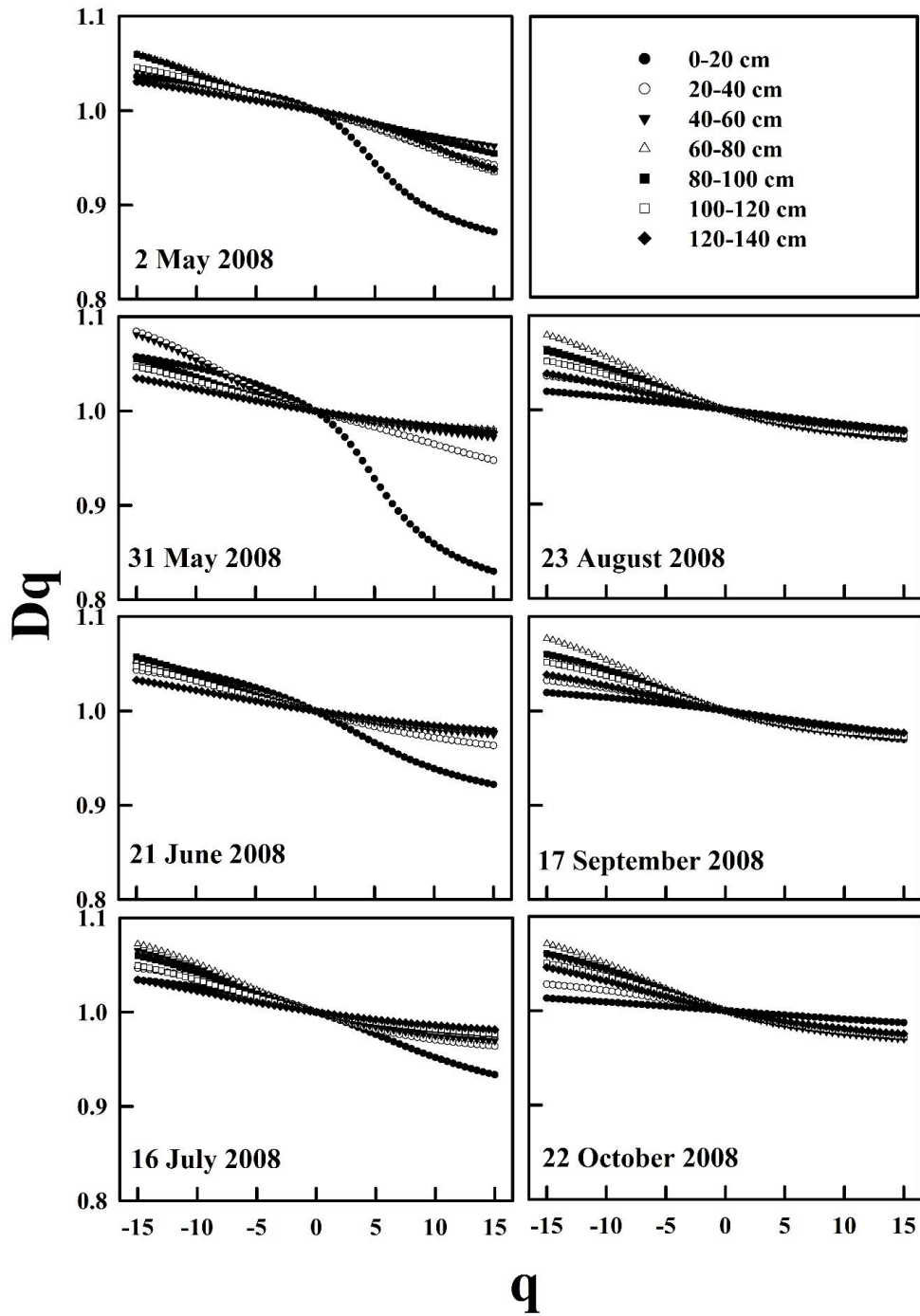
757
758

759 Figure 7



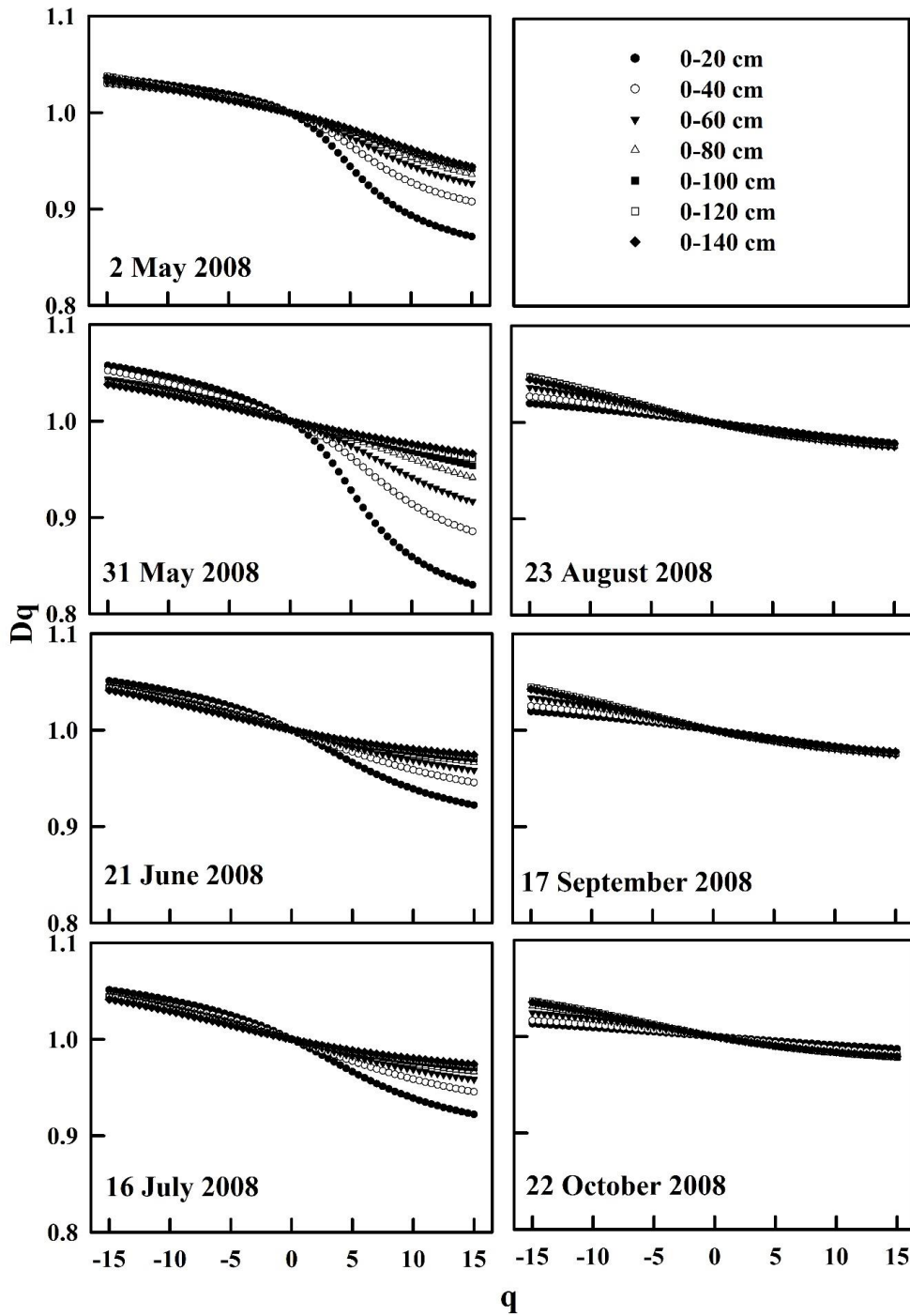
760

761 Figure 8



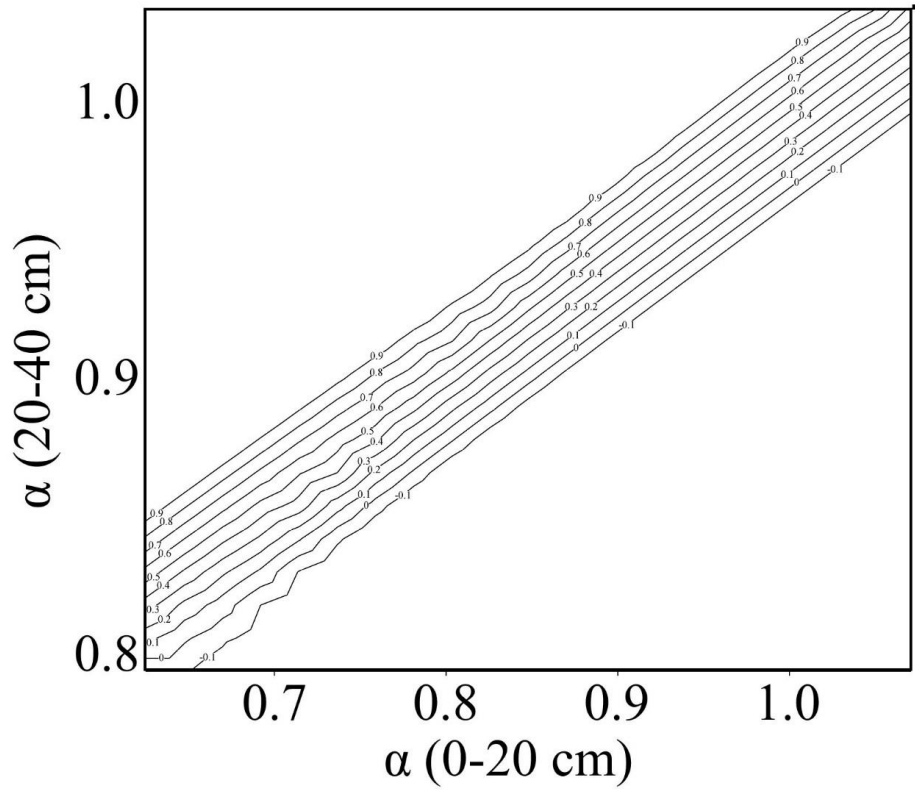
762 Figure 9
763

764



765

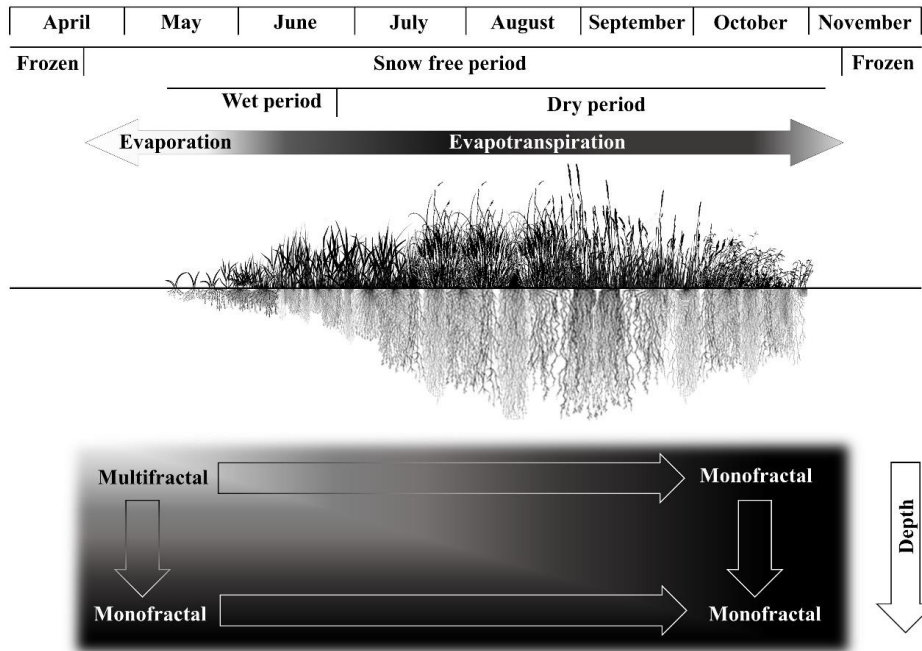
766 Figure 10



767

768 Figure 11

769



770

771 Figure 12